

REPUBLIQUE ALGERIENNE DEMOCRATIQUE ET POPULAIRE

MINISTRE DE L'ENSEIGNEMENT SUPERIEUR
ET DE LA RECHERCHE SCIENTIFIQUE
UNIVERSITE KASDI MERBAH OUARGLA



Faculté des Sciences Appliquées
Département de Génie des Procédés

Mémoire

MASTER ACADEMIQUE

Domaine : Science et Technique

Filière : Génie des Procédés

Spécialité : Génie des pétrochimies

Présenté Par : GHETTAS Imane

Thème :

**Theoretical study on the influence of metal ions doped-CuO
thin films for efficient electrochemical glucose sensor**

Soutenu le : 14/06/2022

Devant le jury :

Dr. Lassouad Ridh	MCA (UKM Ouargla)	Président
Dr. Selloum Djamal	MCA (UKM Ouargla)	Examineur
Dr. Ouidad BAKA	MCB (UKM Ouargla)	Encadreur

Année Universitaire : 2021-2022

Table of contents

Table of contents

<i>Dedication</i>	<i>I</i>
<i>Acknowledgements</i>	<i>II</i>
<i>List of Figures</i>	<i>III</i>
<i>List of Tables</i>	<i>VII</i>
<i>Introduction</i>	<i>1</i>
<i>References</i>	<i>2</i>

Chapter I: Theoretical study on cupric oxide CuO and their doping.

Introduction... ..	3
I.1 Metal oxide thin films	3
I.2 Cupric oxide (CuO).....	4
I.2.1 Properties of Cupric oxide.....	5
I.2.2 Applications of CuO thin films	8
I.3 Doping of semiconductors	9
I.3.1 N doping.....	9
I.3.2 P doping	10
I.4 CuO doping	10
References	20

Chapter II: Metal ions-doped CuO thin films for glucose sensors.

Introduction	22
II.1 Glucose sensors.....	22
II.1.1.Type of glucose sensors	24
II.1.1.1. Enzymatic glucose sensors	24
II.1.2.2 Non-enzymatic glucose sensors	26
II.2 Application of doping CuO in glucose sensors	28
References	47
Conclusion	49

Dedication

To:

The spring of tenderness and safety

Father: Abd erzzak & Mother: warda.

The lights of my eyes

Brothers: Mahdjoub, Abd ennour.

Sisters: Noure elhouda, Marwa, Asma, Nessrine.

My grandmother: Fatma, Nadjma.

*My aunts: Manssoura, Fatiha, Souad, Salima,
Karima, Laila.*

My fiance: Charaf eddin Gana

*My best friends: Ahlam, Chahinaz, Wafa, Safa,
Aicha, Amina, Hayat, Widad, Chaima, Kawter,
Narimane, Hana.*

Everyone who contributed to my success.

Acknowledgements

I would like to express my sincere thanks to my supervisor, Dr. Baka Ouidad, Department of Process Engineering, for all the advice, guidance and support throughout my work on the project. I would like to thank the committee, Dr.Dj. Selloum, Department of Process Engineering And Dr.R.Lassouad, for coming and agreeing to accept arbitration and to examine my work.

I also thank the many people who helped during the five years we spent at the university, and many thanks to our fathers, mothers and all our friends.

Finally, I extend my thanks to all the teachers and students in the Department of Process Engineering, each in his own name.

List of figures

Figure		page
Chapter I: Theoretical study on cupric oxide CuO and their doping		
I.1	Crystal structure of CuO.	6
I.2	Band structure of CuO calculated using (a) the DFT+U method.	7
I.3	(a) Optical transmission spectra of 250 nm thick copper oxide thin films. (b) Tauc plots of copper oxide thin: as deposited, 623 K vacuum annealed and 700 K vacuum annealed.	7
I.4	Applications of CuO: a) solar cells, b) Photo electrochemical cell, c) Gas sensors, d) Photo-catalysis.	8
I.5	N doping semiconductor.	9
I.6	P doping semiconductor.	10
I.7	(a) XRD Measurements, (b) UV-visible spectra of CuO and A doped CuO.	11
I.8	Obtains the UV-VIS absorption spectra of 4-nitrophenol, the addition of the reduction agent (NaBH ₄), and the addition of the prepared CuO thin film and Ag doped CuO thin film.	11
I.9	AFM, 3D image (a, b and c) R_{rms} , R_a and Avg. Diameter for the deposited films.	12
I.10	The energy band gap of the deposited films.	12
I.11	a) XRD patterns. b) Variation of resistivity, mobility, and carrier concentration of spray-deposited CuO:Co thin films with 0 at%, 2 at%, 4 at%, 6 at%, and 10 at% of Co doping.	13
I.12	EDX spectrum of (A) pure CuO and (B) 6% Ba-doped CuO films, (C) Linear sweep voltammetry of the CuO and Ba-doped CuO photo	14

electrodes under white light illumination and (D) reproducible studies of photocurrent density–voltage curves of the 2% Ba-doped CuO photo electrode in the dark and under white light illumination.

I.13	a) Energy band-gap for CuO thin film (C1) undoped. b) Energy band-gap for CuO thin film doping with (CD1) 3%.	15
I.14	Activation energy for CuO pure (C1).	15
I.15	Transient sensor response of the pristine and Cr-doped CuO films Sweat solution was dropped after about 4 min. Response time is less than 60 s until a steady state value is reached. Sensing response is enhanced with Cr-doping.	16
I.16	SEM images of (a) undoped (b) Cd doped CuO (c) Zn doped CuO thin films.	17
I.17	Optical transmittance of undoped and Cd, Zn doped CuO thin films.	18
I.18	Energy band gap of a) pure CuO film, b) 1% Sbdoped CuO film, c) 2% Sb-doped CuO film, d) 3% Sb-doped CuO film.	19

Chapter II: Metal ions-doped CuO thin films for glucose sensors.

II.1	Structures of glucose.	23
II.2	Summary of enzymatic glucose oxidation mechanisms, presented as first, second, and third.	25
II.3	Basic working principle for glucose biosensors.	26
II.4	An illustration of the chemisorption model in glucose oxidation. M: metal atom; C1: hemiacetalic carbon atom; R: other parts of the glucose molecule.	27
II.5	The schematic diagram of incipient hydrous oxide adatom mediator model. M* is the reductive metal adsorption site. M [OH] ads stands for oxidative adsorbed hydroxide radical [12].	27

II.6	Schematic illustration of the synthesis of a non-enzymatic glucose sensor electrode.	28
II.7	(a) CVs of different electrodes at a scan rate of 100 mV/s in 0.1 M NaOH (b) CVs of different electrodes at a scan rate of 100 mV/s in 0.1 M NaOH add 0.1 mM glucose. (c) CVs of the CZF-30 in 0.1 M NaOH containing 1 mM glucose at different scan rates from 20 to 200 mV/s. (d) shows the anodic peak current vs. scan rate.	29
II.8	CV diagrams conducted at a scan rate of 25 mV/s for (a) comparison of the effects of Ni solution on the peak oxidation current and (b) repeatability of N-CuO/Cu ² O: NiO sensor in 1 mM glucose solution.	30
II.9	Amperometric response of: N-CuO/Cu ₂ O, CuO: NiO and CuO: NiO sensor to a, a' and a'') successive additions of glucose, b, b' and b'') corresponding calibration curve including the linear range and c, c' and c'') interference species of biological samples, respectively.	31
II.10	Schematic diagram of the fabrication of the non-enzymatic glucose sensor electrode and its application in glucose detection.	32
II.11	Non-enzymatic detection of glucose. (a) Amperometric response of CuO-ZnO NRs/FTO electrode at +0.62V/Ag/AgCl in 0.1M NaOH solution with different glucose concentration (b) Corresponding calibration plot of current response versus glucose concentration. (c) Anti-interference ability test. Amperometric response of the CuO-ZnO NRs/FTO electrode with the addition of 0.1mM glucose and 0.02Mm of each possible interfering species i.e. (a) AA, (b) UA, (c) DA, (d) NADH, (e) Mg ²⁺ , (f) Ca ²⁺ , (g) Cys, (h) NaCl, (i) lactose, (j) sucrose, (k) maltose, and (l) mannose in the 0.1M NaOH solution at +0.62V (versus Ag/AgCl). (d) Real sample glucose detection. Amperometric response of CuO-ZnO NRs/FTO electrode at +0.62V/Ag/AgCl in 9.5mL 0.1M NaOH solution after injecting 0.5mL blood serum (i) and freshly drawn whole human blood (ii). The upper inset shows the photograph of serum and whole blood samples and lower inset shows the histogram of glucose concentration compared with blood chemistry analyzer result.	33

II.12	Figure.II.12. Schematic of fabrication process of GOx-incorporated PEDOT on the microelectrode array: (a) Pt microelectrode array. (b), (c) Electrodeposition of GOx incorporated PEDOT film. (c) Electrospinning of PLLA nanofibers on the microelectrode array. (d), (f) Electrodeposition of PEDOT around the PLLA nanofibers to form GOx incorporated PEDOT nanofibers. (g) Schematic of entrapment of GOx within PEDOT structure. (h) Optical micrograph of entire microelectrode array. (i) Optical micrograph of microfabricated electrode. (j) SEM of PEDOT F-GOx. (k) Higher magnification SEM of PEDOT FGOx. (l) SEM of PEDOT NFs-GOx. (m) Higher magnification SEM of PEDOT NFs-GOx .	35
II.13	Reaction mechanism of 3D porous ZnO–CuO HNCs electrodes.	36
II.14	The preparation process of Ag/CuO NFs–ITO electrode.	37
II.15	Effect of applied potential on the sensitivity of Ag/ CuO NFs–ITO (Red) and CuO NFs– ITO (black) electrodes to glucose. b) Nyquist plots of Ag/CuO NFs– ITO and CuO NFs–ITO electrodes in 0.10 M KCl solution containing 5.0 mM [Fe (CN) 6]3–/ 4– redox couple. c) Amperometric response of Ag/CuO NFs– ITO and CuO NFs–ITO to successive additions of glucose at an applied potential of 0.50 V. d) Calibration curves obtained from (C).	38
II.16	(a) Schematic illustration of CuO nanostructures evolution; SEM images of CuO ultrafine power with the ratio Cu ²⁺ : OH ⁻ = 1:5 (b); 1:8 (c); and 1:10 (d).	39
II.17	Amperometric response of Nafion/CuO8/GCE and controls to interfering species (a) and sugars (b) at representative physiological concentration levels, respectively.	40
II.18	Figure II.18 (A) CVs of the NiO-MFs modified electrode in the (a) absence and (b) presence 1 mM of glucose in 0.1 M of NaOH; (B) CVs	41

of the CuO-NiO-MFs modified electrode in (a) absence and (b) presence 1 mM of glucose in 0.1 M of NaOH; (C, D) CVs of the NiO-MFs and CuO-NiO-MFs modified electrode, respectively, in 0.1 M of NaOH with (a) 1, (b) 2, (c) 3, and (d) 4 mM of glucose, scan rate fixed at 50 mVs⁻¹ [16].

- II.19** **Figure II.19** (A) Amperometric response of (a) the NiO-MFs and (b) the CuO-NiO-MFs modified electrode upon successive addition of glucose at 0.03 mM to 0.1 M of NaOH at an applied potential of 0.5V; (B) the calibration curve for the amperometric response of the CuO-NiO-MFs modified electrode;(C) amperometric response of the CuO-NiO-MFs modified electrode with successive 3-time addition of analytes in the sequence of 4 L of blood serum sample, 4 L 4 mM of glucose, 8 L of blood serum sample and 8 L 4 mM of glucose in 0.1 M of NaOH solution [16]. **42**
- II.20** (A) Amperometric response of the CuO-NiO-MFs modified electrode with successive 4-time additions of interferences in the sequence of 0.3 M of DA, 0.3 M of AA, 0.3 M of glucose and 3 M of glucose in 0.1 M of NaOH solution; (B) stability of the CuO-NiO-MFs modified electrode stored at ambient conditions over 15-day periods in the presence 2 mM of glucose in 0.1 M of NaOH solution. **43**
- II.21** a) XRD patterns of the products and b) XPS spectra of Pd 3d for PCNFs. **44**
- II.22** Cyclic voltammograms (CVs) of 0.6 mM glucose in 0.1 M NaOH. **45**

List of Tables

Table		page
I.1	Some metal oxides, their position in the periodic table, band gap and conducting nature	4
I.2	Physical properties of CuO	5
I.3	Crystallographic properties of CuO	6
Chapter II: Metal ions-doped CuO thin films for glucose sensors.		
II.1	Sensors based on their detection properties	24
II.2	A performance comparison of CuO thin films.	46

Introduction

Introduction

Nano-materials and nanotechnology have attracted great attention in recent research. New physical properties and new technologies both in sample preparation and device fabrication evoke on account of the development of nano-science. The research involved several fields of study, including physicists, chemists, materials scientists, and mechanical and electrical engineers [1]. At present, research on nano-materials is intensified and is expanding rapidly. In addition, metal oxide nano-materials have drawn a particular attention because of their excellent structural flexibility combined with other attractive properties [2]. One of those interesting metallic oxides is cupric oxide (CuO). CuO is a p-type semiconductor with inherent advantageous properties such as low production cost, non-toxicity, and abundance of the constituent materials [3]. In addition, to improve the CuO's properties, several researchers have based on the insertion of metal ions such as Fe, Mn, Zn, W and Mg into the crystal lattice of this oxide (doping) [4]. CuO nano-materials offer great potential for the development of electrode materials for the non-enzymatic electrochemical determination of glucose. They also exhibit high sensitivity, stability and fast response for glucose detection due to their excellent catalytic and electrochemical capabilities [5].

This work focuses on the effect of metal ions doped copper oxide thin films. The purpose this study is the improvement of the CuO thin films properties during doping and its applications for an efficient electrochemical glucose sensor. This work is divided into two chapters comprising a general introduction and a conclusion.

In the first chapter, we presented the copper oxide properties and their applications in modern technologies. Then we discussed the concept of semiconductors followed by metal oxides. Finally, it will be presented doping CuO.

In the second chapter, we focus our attention on CuO thin films in medical fields such as detection of glucose, we presented also the types of glucose sensors, and application of CuO doping in glucose sensors.



References

- [1] J.T.Lue, «*Physical Properties of Nanomaterials, Encyclopedia of Nanoscience and Nanotechnology*», Edited by H. S. Nalwa, Volume X (2007) Pages (1–46)
- [2] S. Zaman, «*Synthesis of ZnO, CuO and their Composite Nanostructures for Optoelectronics, Sensing and Catalytic Applications*», Linköping University, Physical Electronics and Nanotechnology Department of Science and Technology (2012)
- [3] S. Dolai, R. Dey, S. Das, S. Hussain, R. Bhar, A.K. Pal, «*Cupric oxide (CuO) thin films prepared by reactive d.c. magnetron sputtering technique for photovoltaic application*», *Journal of Alloys and Compounds*, 724 (2017) 456-464
- [4] Z. Zhuang, X. Su, H. Yuan, Q. Sun, M.M.F. Choi, «*An improved sensitivity nonenzymatic glucose sensor based on a CuO nanowire modified Cu electrode*» , (2008) 126–132.
- [5] A. Inyang, G. Kibambo, M. Palmer, F. Cummings, M. Masikini, C. Sunday, M. Chowdhury, «*One step copper oxide (CuO) thin film deposition for non-enzymatic electrochemical glucose detection*», *Thin Solid Films*, 709 (2020) 138244.

Chapter I:
Theoretical study on
cupric oxide CuO and
their doping

Thin film technology is one of the oldest arts and the latest in science. Recently, copper oxide is considered an important category in many applications of nanotechnology. This chapter covers a brief survey of the most important properties of thin films and their applications in various fields of technology. Moreover, some modifications were made to the metal surface by changing its size and shape by adding copper oxide doped with other different and suitable materials.

I.1 Metal oxide thin films

Metal oxides in general are chemical compounds containing one or more metals and oxygen, which are very important for scientific and technological requirements. Metal oxide films have been known many times due to the structural interest for their unique and distinctive properties. The latter plays an important role in the physical and chemical fields because its properties are closely related to the preparation process. Adapting the electrical, structural and optical properties of the films by changing the state and deposition process, so the properties are the main parameters for preparing metal oxide films. Earlier research was in the field of bulk metal oxides before paying attention to the side of thin films, including (ZnO, SnO₂, TiO₂, WO₃, Cu₂O, and CdO). Various metal oxide thin films have recently appeared, including copper oxide thin films, which are interesting for their multiple properties, including optical, semiconductor, magnetic, electronic and optoelectronic. The table shows the nature of different metal oxides [1].

Table I.1 Some metal oxides, their position in the periodic table, band gap and conducting nature [1].

Name	Position of the metal in the periodic table and nature	Band gap (eV)	Classification
WO₃	Group 6 (IV) : transition metal	2.6-3.1	Semiconductor (n-type)
MnO	Group 7 (IV) : transition metal	4.1	Semiconductor (n-type)
Mn₃O₄	Group 7 (IV) : transition metal	2.5	Semiconductor (n-type)
MnO₂	Group 7 (IV) : transition metal	β 0.26 - γ 0.58-0.7	Semiconductor (n-type)
FeO	Group 8 (IV) : transition metal	2.4-2.5	Semiconductor (n-type)
Fe₃O₄	Group 8 (IV) : transition metal	0.1	Metallic
Fe₂O₃	Group 8 (IV) : transition metal	α 2.2- γ 2.0	α = Semiconductor (n-type) γ = Semiconductor (n-type)
RuO₂	Group 8 (V) : transition metal	2.2	Semiconductor (Amphoteric)
CoO	Group 9 (IV) : transition metal	2.4	Semiconductor (p-type)
Co₃O₄	Group 9 (IV) : transition metal	2.0-0.2	Semiconductor (p-type)
NiO	Group 10 (IV) : transition metal	3.6-4.2	Semiconductor (p-type)
CuO	Group 11 (IV) : transition metal	1.2-2.2	Semiconductor (p-type)
Cu₂O	Group 11 (IV) : transition metal	2.1-2.2	Semiconductor (p-type)
ZnO	Group 12 (IV) : poor metal	3.3-3.4	Semiconductor (p-type)
CdO	Group 12 (V) : poor metal	2.2-2.9	Semiconductor (n-type)
Al₂O₃	Group 13 (III) : poor metal	6.0-8.8	Semiconductor (n-type)
Ga₂O₃	Group 13 (IV) : poor metal	β 4.7-4.9	Semiconductor (n-type)

I.2 Cupric oxide (CuO)

CuO is one of oldest known semiconductor due to these unique features such as low cost, non-toxicity and the abundant availability of copper in nature. CuO Thin films have been intensely studied as a promoting material for many industrial applications [2].

CuO thin film has a relatively low band gap (1.2-1.9 eV); it is very important p-type semiconductor with a monoclinic structure. CuO base materials have found special interest for several applications such as photo-catalysis, magnetic storage, gas sensor and solar cells [2].

I.2.1 Properties of Cupric oxide

Copper oxide has several good and useful properties in all studies, which are as follows:

I.2.1.1 Physical and chemical proprieties

Copper oxide is a black solid powder with a density of 6.32 and a melting point of 1134 °C with some loss of oxygen, and it is insoluble in water. Table I.2 regroups some physical and chemical properties of cupric oxide [1].

Table I.2 Physical properties of CuO [1].

Cupric oxide (CuO)	
Chemical names	copper (II) oxide
	cupric oxide
	copper monoxide
	copper oxide (CuO)
	Oxocopper
Molecular formula	CuO
Appearance	black powder
Solubility in water	Insoluble
Molecular mass	79.55 (g/mol)
Density	6.32 (g/cm ³)
Melting point	1134° c
Boiling point	2000° c
Relative permittivity	12

I.2.1.2 Crystal structure of cupric oxide

The copper oxide crystal has a monoclinic structure, containing four CuO molecules (as shown in Figure I.1). The coordination number of a copper atom is 4, which means that it is bonded to four neighboring atoms of oxygen in a roughly square planar configuration in the (110) plane. Each atom of copper is associated with Four O atoms. Whereas, each O atom is coordinated to four copper atoms in disorder tetrahedron.

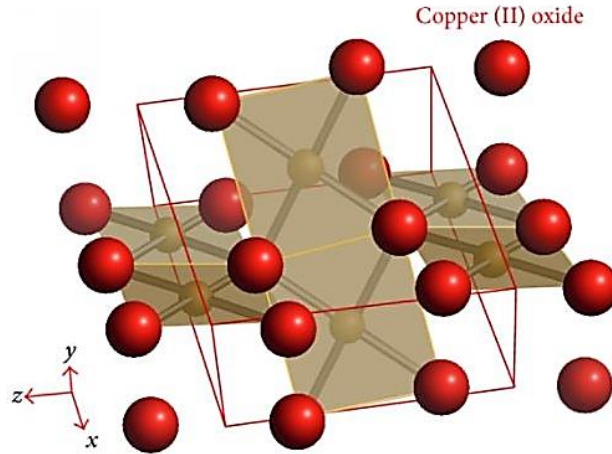


Figure I.1 Crystal structure of CuO [3].

Lattice constants and other crystallographic properties are listed in Table (I.3) [3].

Table I.3 Crystallographic properties of CuO [3].

Crystallographic properties of CuO	
Space group	C2/c
Unit cell	a = 4.6837 Å
	b = 3.4226 Å
	c = 5.128 Å
	$\beta = 99.548^\circ$
	$\alpha, \gamma = 90^\circ$
Cell volume	81.08 Å ³
Cell content	4 [CuO]
Distances	
Cu-O	1.96 Å
Cu-Cu	2.62 Å
O-O	2.90 Å

I.2.1.3 Electronic properties of cupric oxide

Cupric oxide (CuO) is a direct band gap semiconductor with the smallest band gap at the center of Brillouin zone Γ , showing the electronic structure of CuO in the monoclinic structure. The calculation using Density Function Theory (DFT) in located density approximation found

a band gap values of 1.251 eV which is in agreement with the experimentally measurements reported at ambient temperature indicating a band gap values in the range 1.2 to 1.9 eV [4].

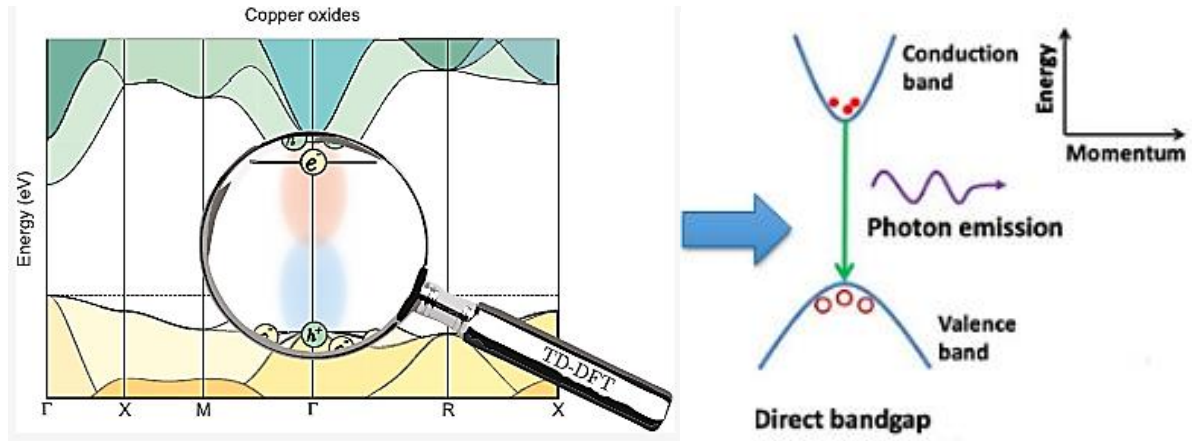


Figure I.2 Band structure of CuO calculated using (a) the DFT+U method.

I.2.1.4 Optical properties

Optical properties are a pivotal parameter of thin-film optoelectronics. The importance of CuO optical parameters started from their beneficial processes such as the absorbent sublayer in solar cells. This process requires high immersion in the visible range of the sun.

Regardless of the deposition technique, CuO thin films have a transparency ranged from 0 to 80%. Sedimentation technique and experimental parameters affect the structural properties, film surface morphology, and optical properties change by the preparation conditions.

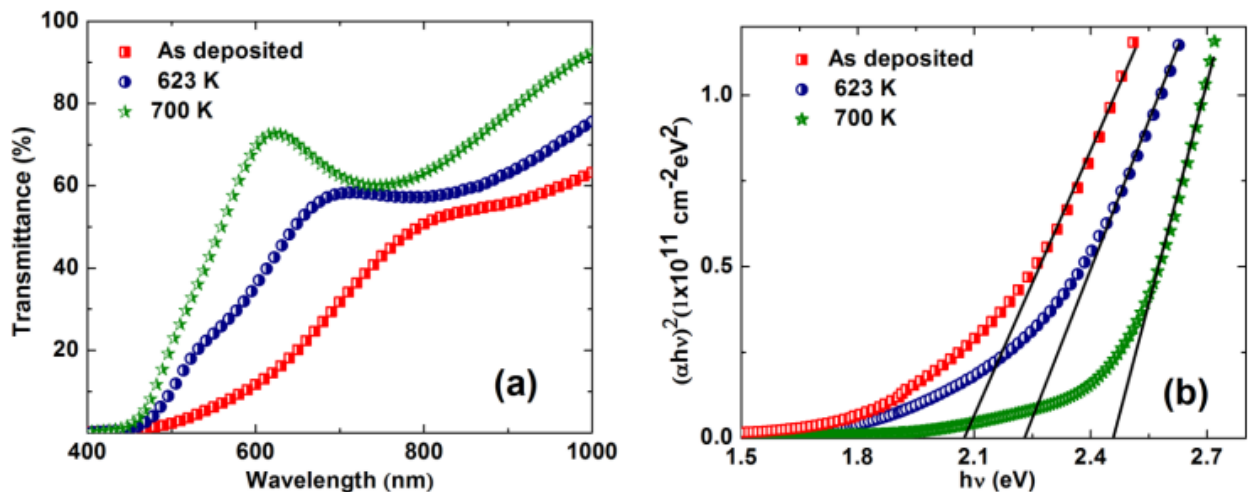


Figure I.3 (a) Optical transmission spectra of 250 nm thick copper oxide thin films. (b) Tauc plots of copper oxide thin: as deposited, 623 K vacuum annealed and 700 K vacuum annealed [5].

I.2.2 Applications of CuO thin films

Due to the availability of many of these applications and their components in nature, with low cost, good thermal stability and electrochemical properties. This composite property of copper oxide thin films has also made it possible to have good efficiency for many applications namely: high-temperature superconductors, solar cells, gas sensors, magnetic storage media varistors, catalysis, antimicrobial activity, photo electrochemical cell and Li batteries [1].

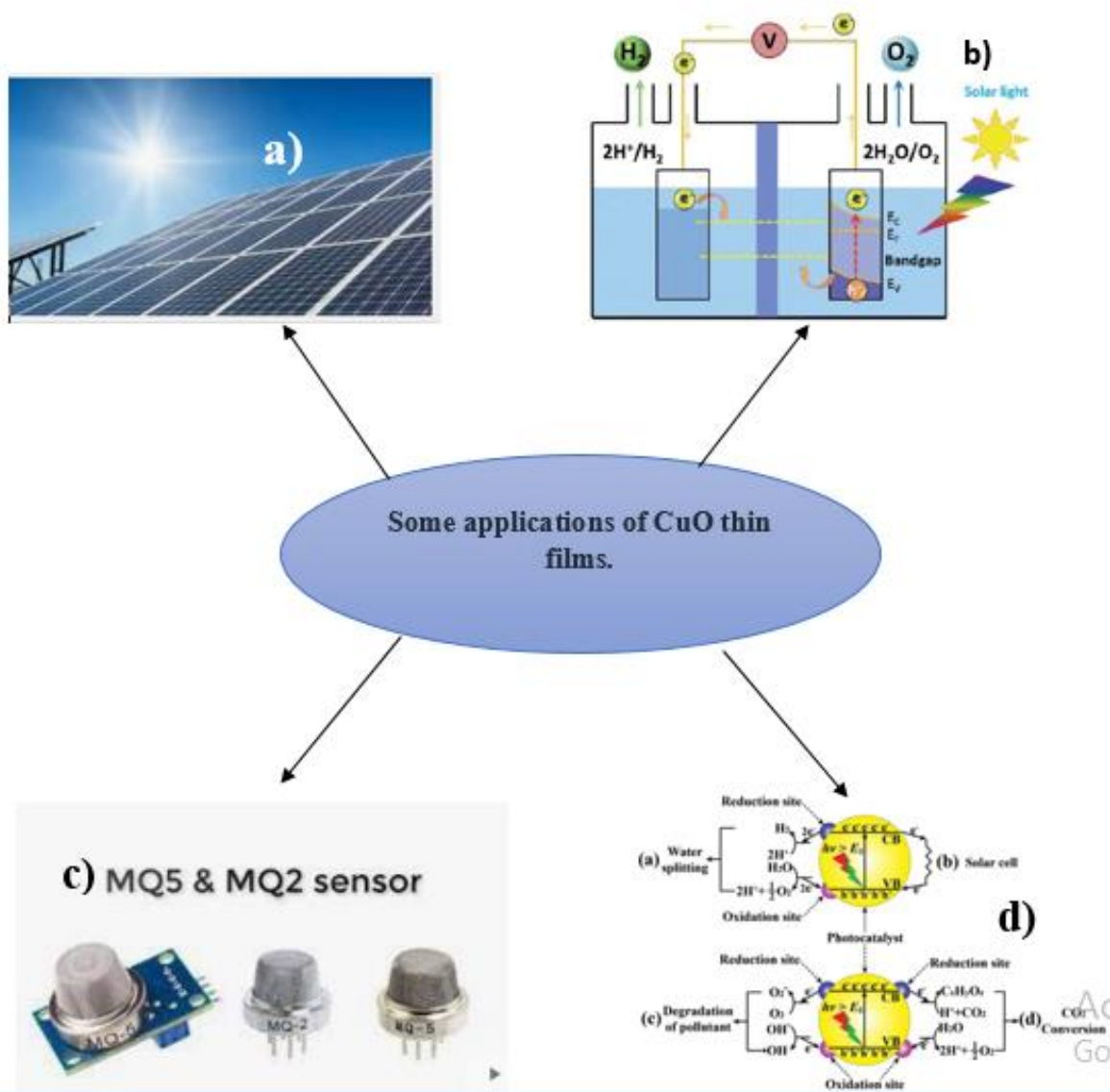


Figure I.4 : Applications of CuO: a) solar cells, b) Photo electrochemical cell, c) Gas sensors, d) Photo-catalysis.

I.3 Doping of semiconductors

In semiconductor production, doping refers to the process of intentionally introducing impurities into an extremely pure (also referred to as intrinsic) semiconductor in order to change its electrical properties. The impurities are dependent upon the type of semiconductor. Lightly and moderately doped semiconductors are referred to as extrinsic. A semiconductor which is doped to such high levels that it acts more like a conductor than a semiconductor is called degenerate [6].

The doping with donors and acceptors allows to modify the electron and hole concentration in silicon in a very large range from 10^{13}cm^{-3} up to 10^{21}cm^{-3} . The carrier concentration can also be varied spatially quite accurately which is used to produce pn-junctions and built-in electric fields. All electronic and optical semiconductor devices incorporate dopants as a crucial ingredient of their device structure [7].

I.3.1 N doping

This involves substituting Si by neighboring elements that contribute excess electrons. For example, small amounts of P or As can substitute Si. Since P/As have 5 valence electrons, they behave like Si plus an extra electron. This extra electron contributes to electrical conductivity, and with a sufficiently large number of such dopant atoms, the material can display metallic conductivity. With smaller amounts, one has extrinsic n-type semiconduction [8].

The donor levels created by substituting Si by P or As lie just below the bottom of the conduction band. Thermal energy is usually sufficient to promote the donor electrons into the conduction band [9].

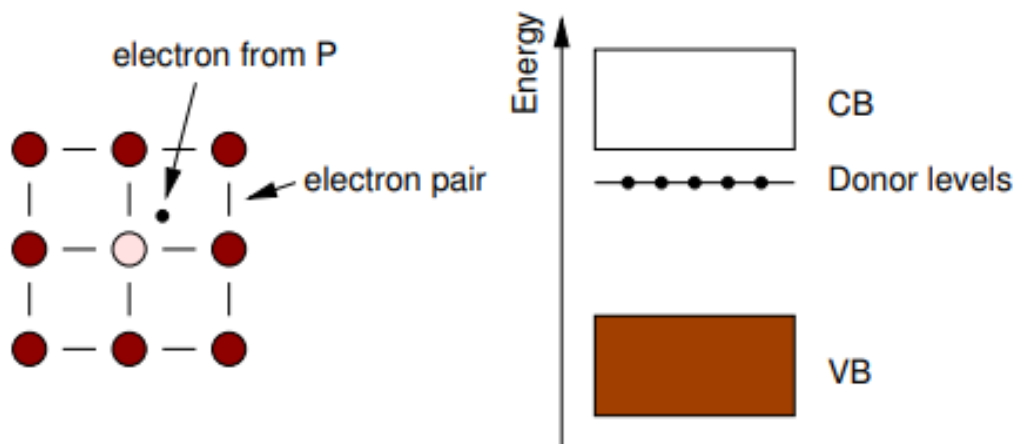


Figure I.5 N doping semiconductor.

I.3.2 P doping

This involves substituting Si by neighboring atom that has one less electron than Si, for example, by B or Al. The substituent atom then creates a “hole” around it that can hop from one site to another. The hopping of a hole in one direction corresponds to the hopping of an electron in the opposite direction. Once again, the dominant conduction process is because of the dopant [8].

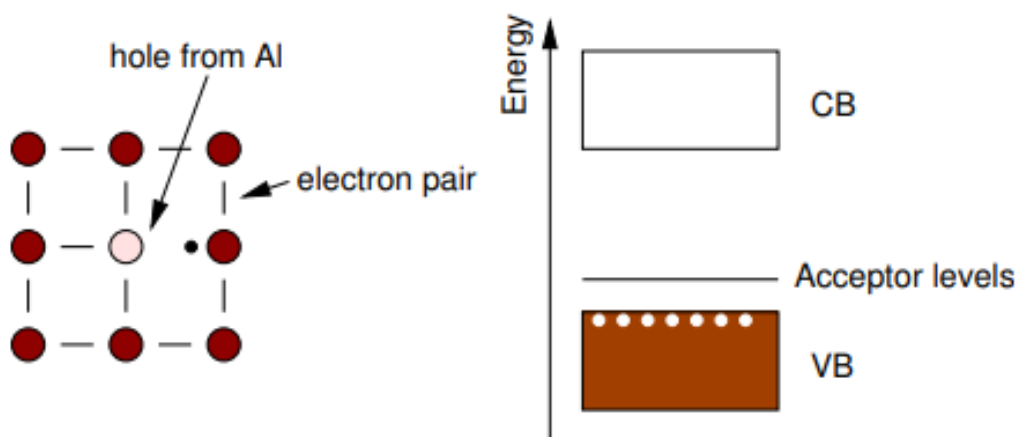


Figure I.6 P doping semiconductor.

I.4 CuO doping

In order to improve the performance of thin films of copper oxide, some researchers resorted to the use of doping of metal ions as recorded in the text.

A. A Menazea et al. were used pulsed laser deposition (PLD) technique for deposited silver-doped copper Oxide thin film as high activity catalytic sheet for degradation of 4-nitrophenol. The synthesized Silver doped Copper Oxide thin film has been characterized via various spectroscopic techniques. XRD measurements confirm the improvement crystallinity of CuO thin film after doped by Ag. From the (figure I.7.a), UV-visible spectra approved the increasing in the values of transmittance of CuO doped by Ag thin film. The obtained direct band gap value of pure CuO thin films is 2.64 eV, which decreases to 2.43 eV after the doping by Ag. (Figure I.7.b) [10].

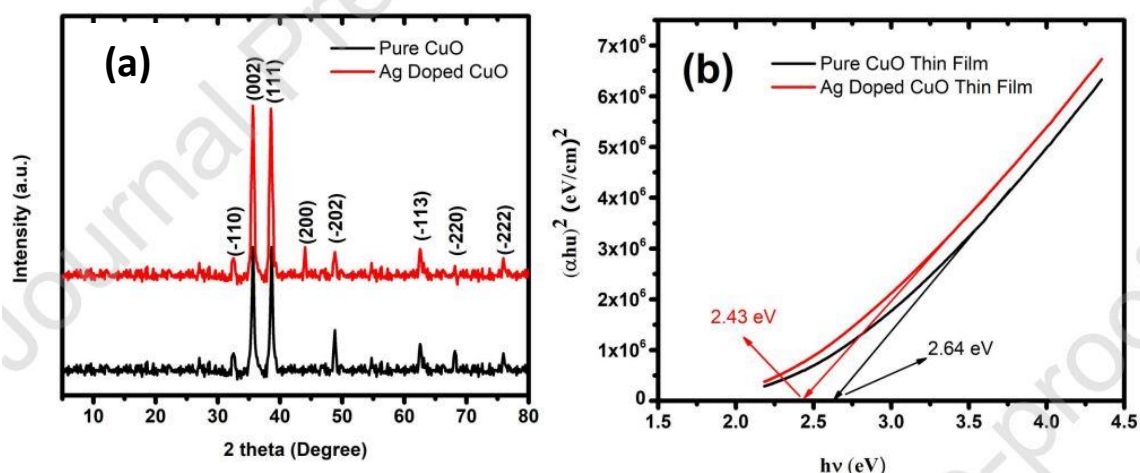


Figure I.7 (a) XRD Measurements, (b) UV-visible spectra of CuO and A doped CuO [10].

The catalytic performance of 4-nitrophenol degradation via CuO has been improved after doping by Ag via PLD according decreasing the time of the total degradation from 60 min to 25 min(figure I.8) The stability of the enhanced thin film confirms its possibility to use for 10 cycles and still highly efficient. The design and construction of such as this thin film consider a high impact for the removal of dyes from wastewater [10].

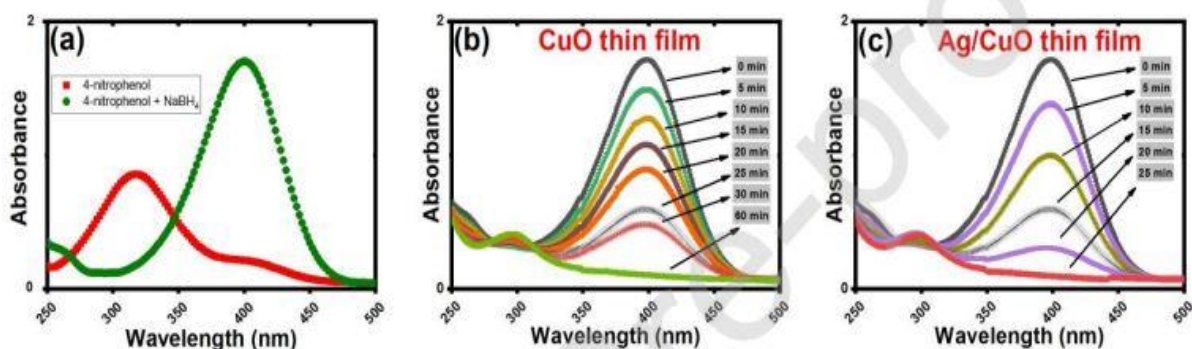


Figure I.8 Obtains the UV-VIS absorption spectra of 4-nitrophenol, the addition of the reduction agent (NaBH₄), and the addition of the prepared CuO thin film and Ag doped CuO thin film [10].

In another hand, H.A. Hussin et al. were prepared nanostructured copper oxide (CuO) doped with Mn thin films at varying doping (2% and 4%) by chemical spray pyrolysis (CSP) technique. XRD was used to characterize structural properties confirms that films were polycrystalline with a preferred orientation along (002) plane. Films morphology was evaluated via Atomic Force microscopy (AFM) (Figure I.9) [11].

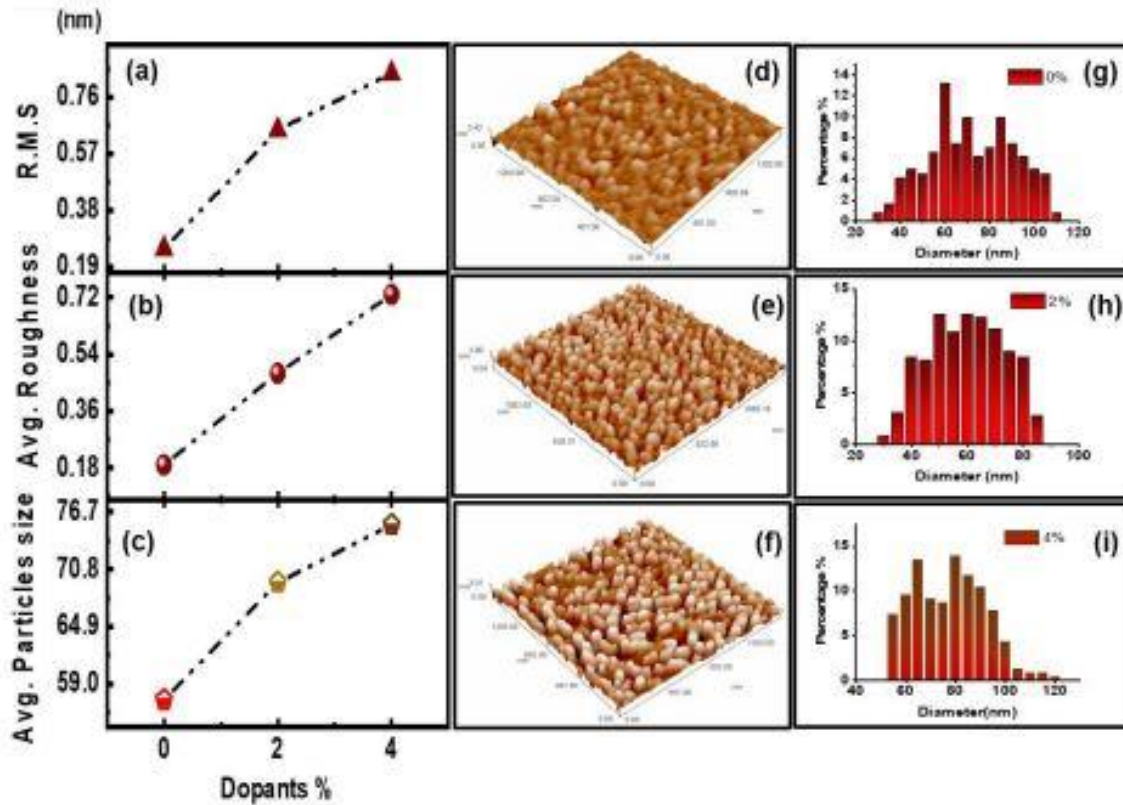


Figure I.9 AFM, 3D image (a, b and c) R_{rms} , R_a and Avg. Diameter for the deposited films [11].

Optical properties were obtained via spectrophotometer and the results indicate that CuO and Mn doped CuO Nanostructured have a range of band gap values within (1.72 - 1.92) eV (Figure I.10). The relationship between the optical and electrical properties is very strong, when the charge carrier concentrations up the resistivity of the films reducing [11].

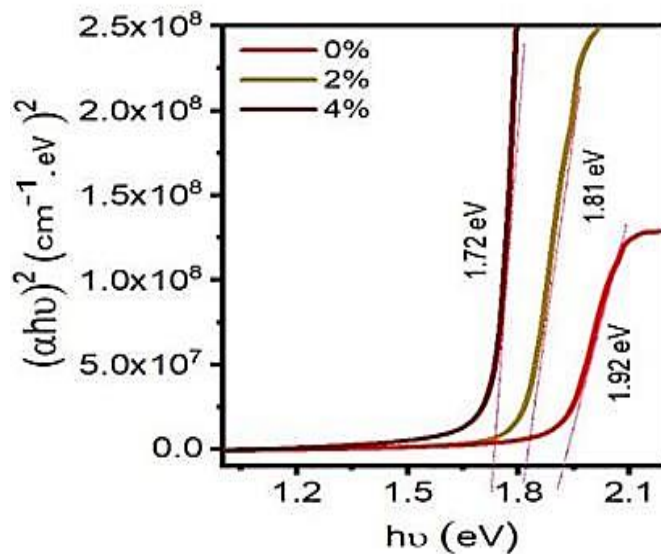


Figure I.10 The energy band gap of the deposited films [11].

H. Z. Asl et al. has studied the structural, morphological, electrical and optical properties of nanostructured copper oxide (CuO) films deposited by spraying deposited on cobalt (Co)-doping (0 at %, 2% at %, 4% at %, 6% at %, and 10 in%). Where X-rays revealed a decrease in the size of the crystals when the concentration of cobalt increased (figure I.11.a). Doping turns a weak p-type conductor into a large n-type conductor. The large increase in free electron appears to be the carrier attention is responsible for the conductivity transmission and its enhancement (figure.I.11.b) [12].

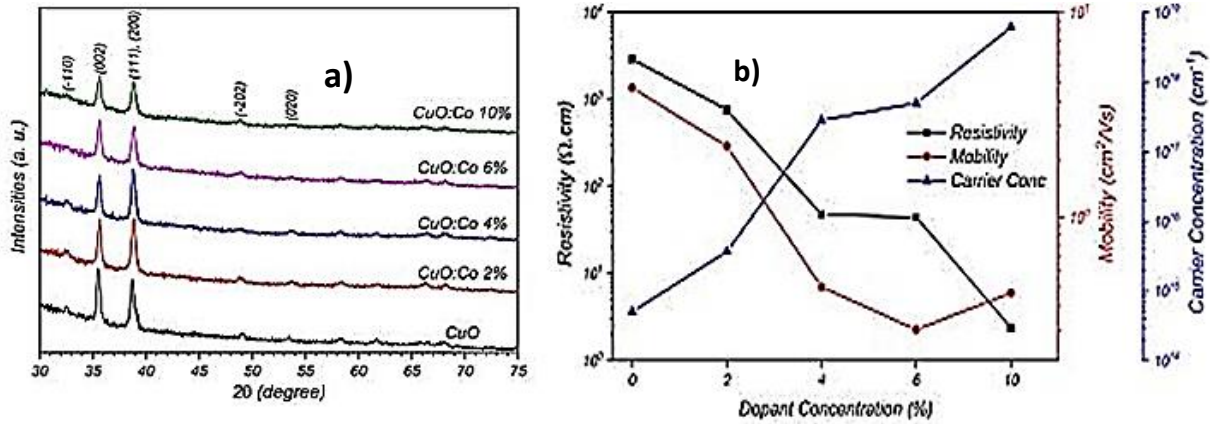


Figure I.11 a) XRD patterns. b) Variation of resistivity, mobility, and carrier concentration of spray-deposited CuO:Co thin films with 0 at%, 2 at%, 4 at%, 6 at%, and 10 at% of Co doping[12].

In this work, A. M. Ahmed et al. prepared CuO and Ba-doped CuO thin films on glass substrates using simple successive ionic layer adsorption and reaction method (SILAR) to produce hydrogen. Band gap films between 1.63eV and 1.87eV were detected to control the ratio of doping after incorporation 6%. An increase in doping leads to a decrease in the particle size. The dispersive X-rays of the high transmittance energy of the precipitated films showed the appearance of a layer of Ba after increasing the doping ratio, giving a value of 0.21 and 0.82 at 6% (figure .I.12.A and B) .The 2% Ba- un-ravel CuO flicks showed a high photo-catalytic performance as a photo electrode for effective hydrogen generation (figure .I.12.C and D). Hence, the 2 %Ba- doped CuO photo electrode can be used as an effective and low- cost photo electrode for solar hydrogen product [13].

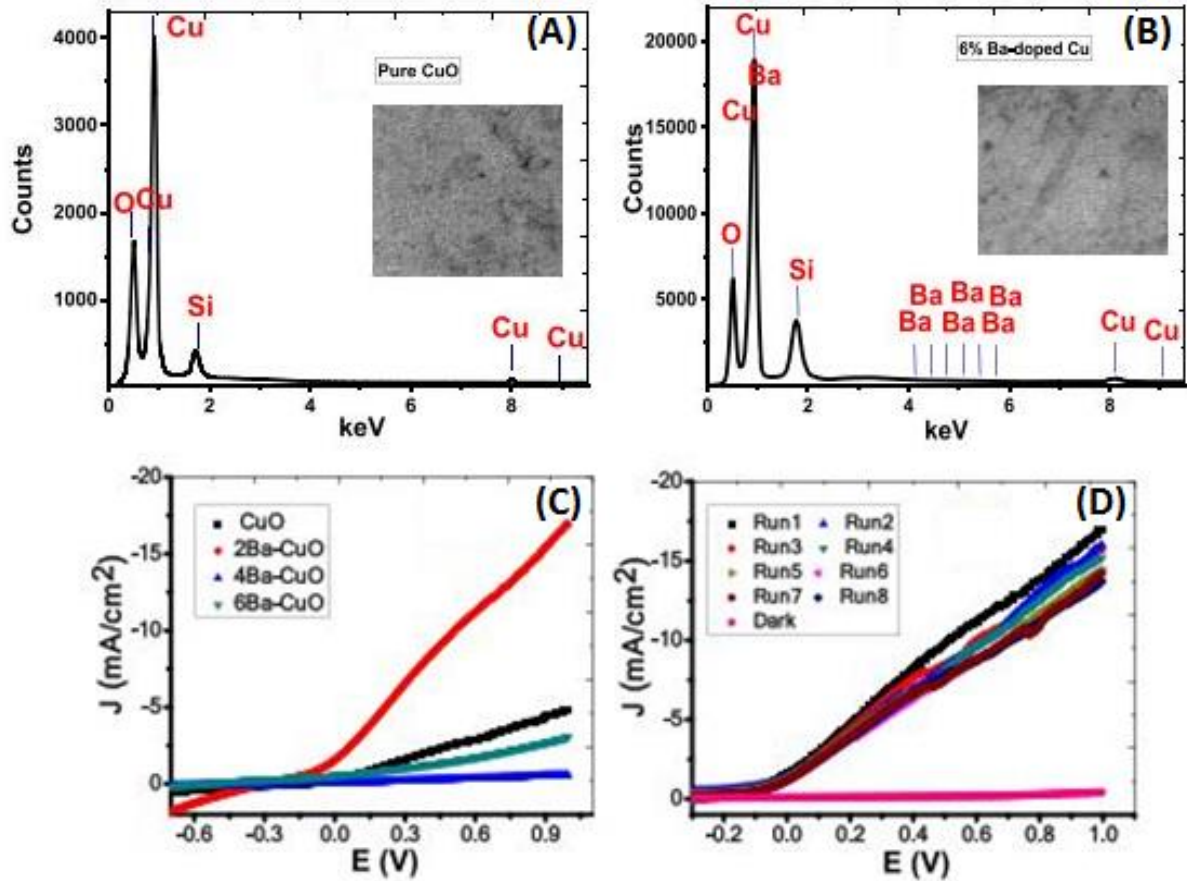


Figure I.12 EDX spectrum of (A) pure CuO and (B) 6% Ba-doped CuO films, (C) Linear sweep voltammetry of the CuO and Ba-doped CuO photo electrodes under white light illumination and (D) reproducible studies of photocurrent density–voltage curves of the 2% Ba-doped CuO photo electrode in the dark and under white light illumination[13].

A. N. Hussain et al. were deposited thin films of doped copper (II) oxide (COTF) by chemical spray pyrolysis method. COTF is deposited on a silicon substrate to fabricate heterogeneous CuO-Si. Structural analyses have confirmed monoclinic polycrystalline for COTF deposited at 400 °C substrate temperature. Compared with pure COTF, Co-doped samples showed larger grain size with deformation in the structure. With the increase of doping attention, the structure changes to unformed. Band gap energy was 2.45 eV before doping and 2.6 eV at 3% doping and began to drop with adding doping attention (figure.I.13) [14].

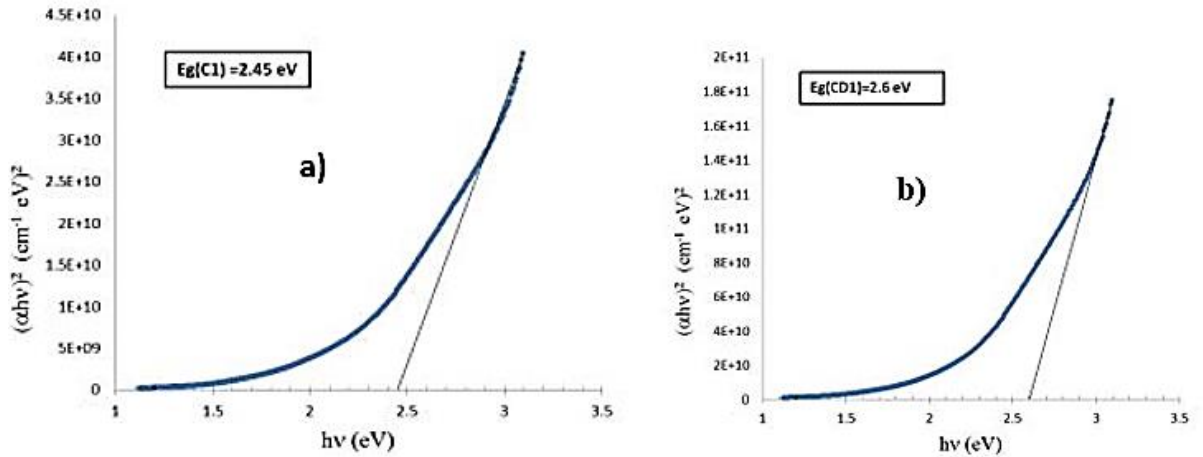


Figure I.13 a) Energy band-gap for CuO thin film (C1) undoped. b) Energy band-gap for CuO thin film doping with (CD1) 3% [14].

Activation energy was be 0.24 eV and it drop with increase of doping (figure.I.14)

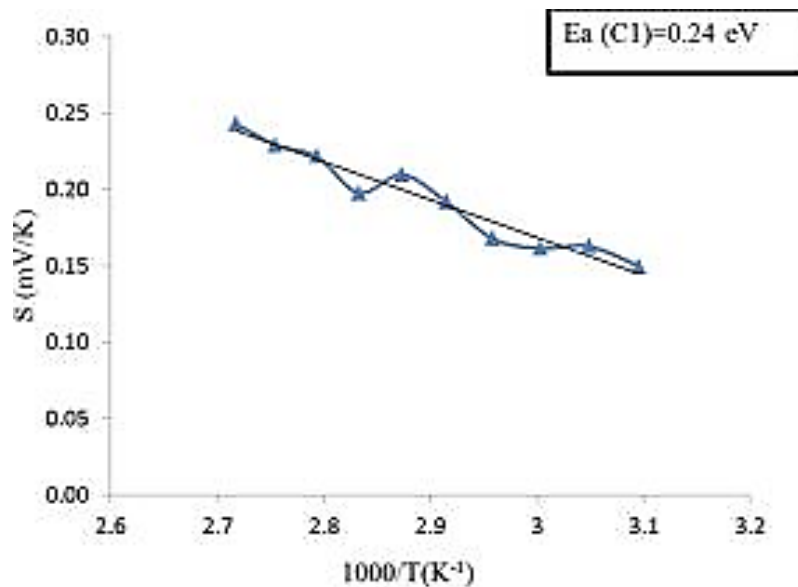


Figure I.14 Activation energy for CuO pure (C1) [14].

In another hand, S. Dinc et al. we have studied the effect of chromium doping of CuO on the main physical properties and hydration level sensing ability of thin-film samples synthesized by SILAR method on soda-lime glass substrates. Doping with chromium increases the sweat sensing performance of copper oxide films. We have conducted several analysis to corroborate the Cr doping into CuO including face morphology and essential identification through SEM and EDX, liquid structure analysis through XRD, and optic analysis via UV – Vis. Results have shown that CuO was successfully unravel with Cr without altering the integrity of the demitasse. Doping improves the sweat sensing response of the metal oxide membranes (sensing response from 0.45 to 8.50 for heavy doping) (figure.I.15). We conclude

that Cr-doping improves the sensing performance of CuO thin films and offers to be implemented in sweat sensing devices as the sensing material [15].

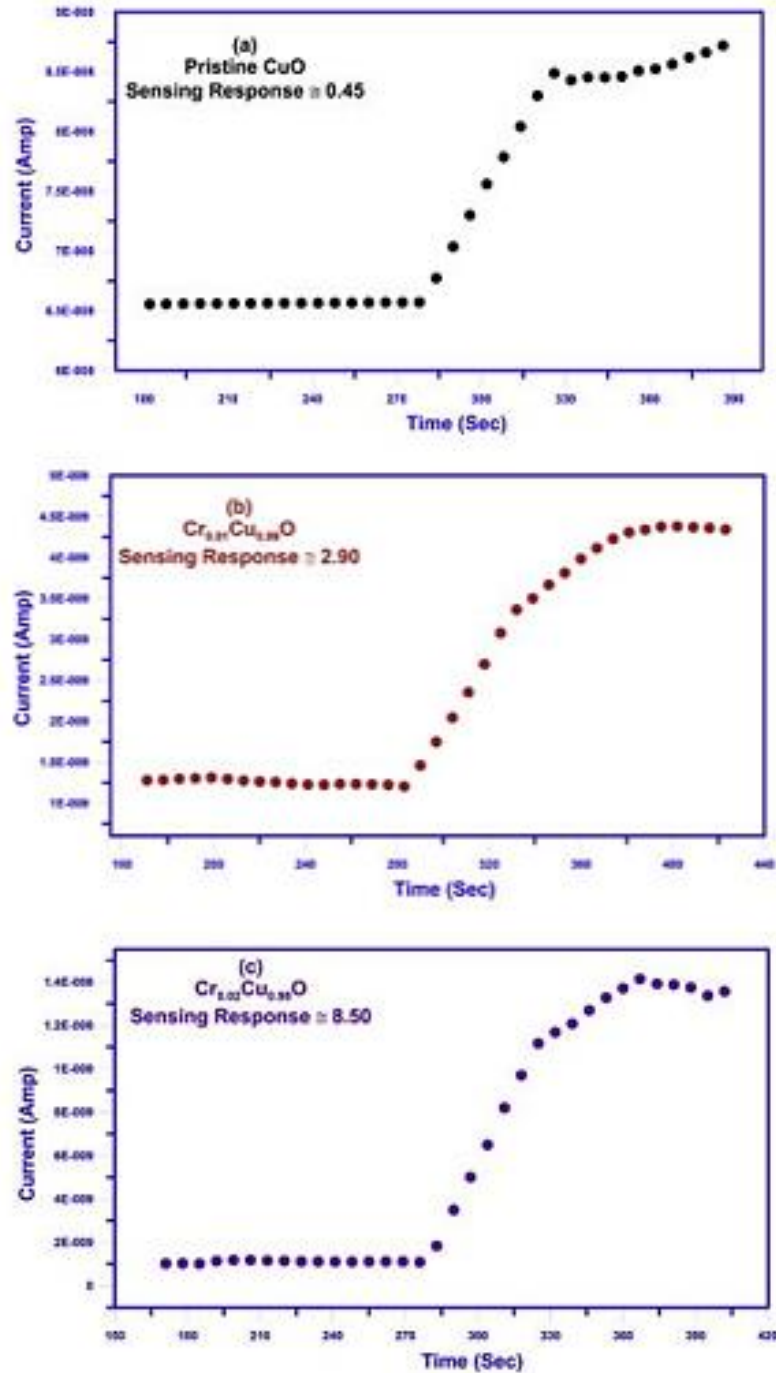


Figure I.15 Transient sensor response of the pristine and Cr-doped CuO films Sweat solution was dropped after about 4 min. Response time is less than 60 s until a steady state value is reached. Sensing response is enhanced with Cr-doping [15].

S.J. Helen et al. prepared CuO (uncoated) zinc-cadmium thin films by spraying Pyrolysis technic on glass substrates. X ray diffraction (XRD) analysis exposes that the prepared pure and Zn and Cd doped CuO films show polycrystalline nature with face centered cubic structure.

In addition, Zn and Cd doping radically increases the crystalline and changes the crystallite size. SEM images illustrate that the surface morphology was formed by grains, which are rod shaped grains uniformly distributed (figure.I.16) [16].

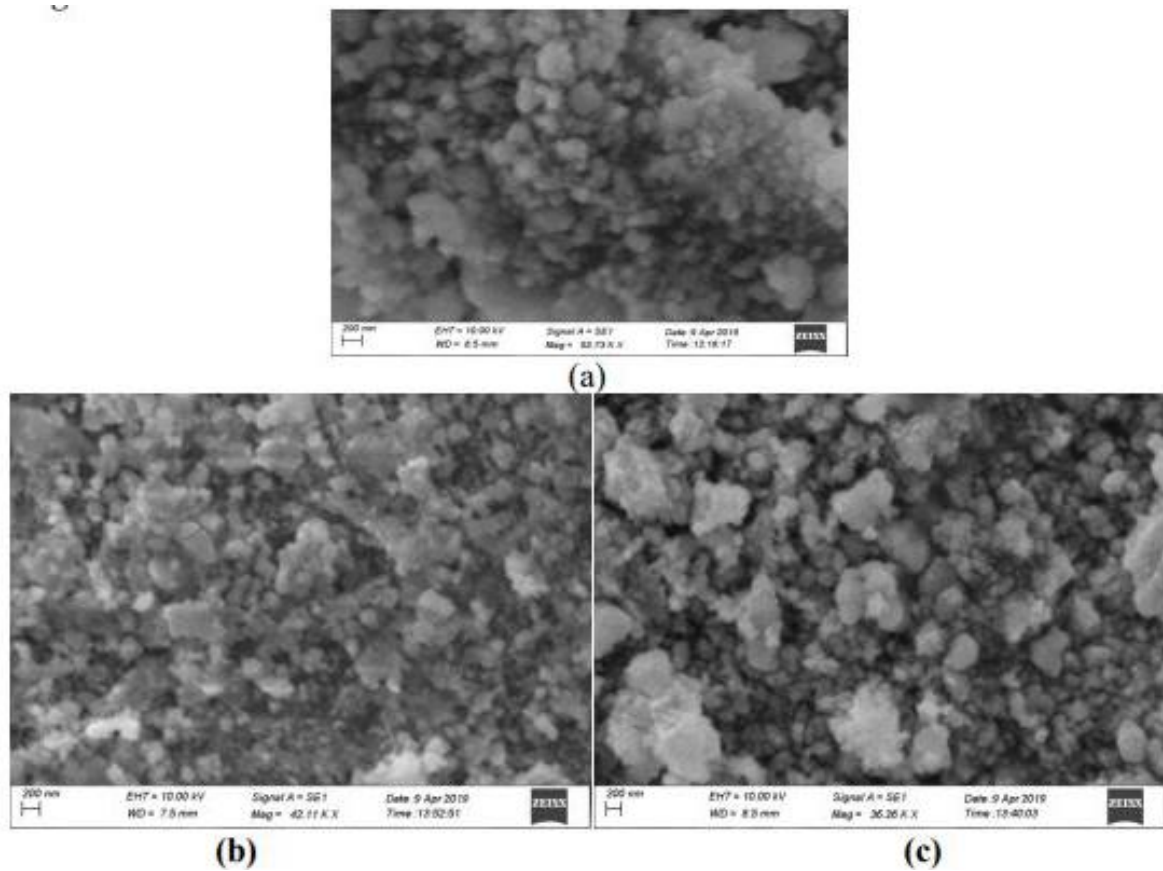


Figure I.16 SEM images of (a) undoped (b) Cd doped CuO (c) Zn doped CuO thin films.

The transmittance of the prepared CuO films recorded in the UV visible spectra show 40 to 70% in the visible region (figure.17). Also, it is experiential that when the Cd doped, the electrical resistivity is high when compared to Zn doped CuO thin films [16].

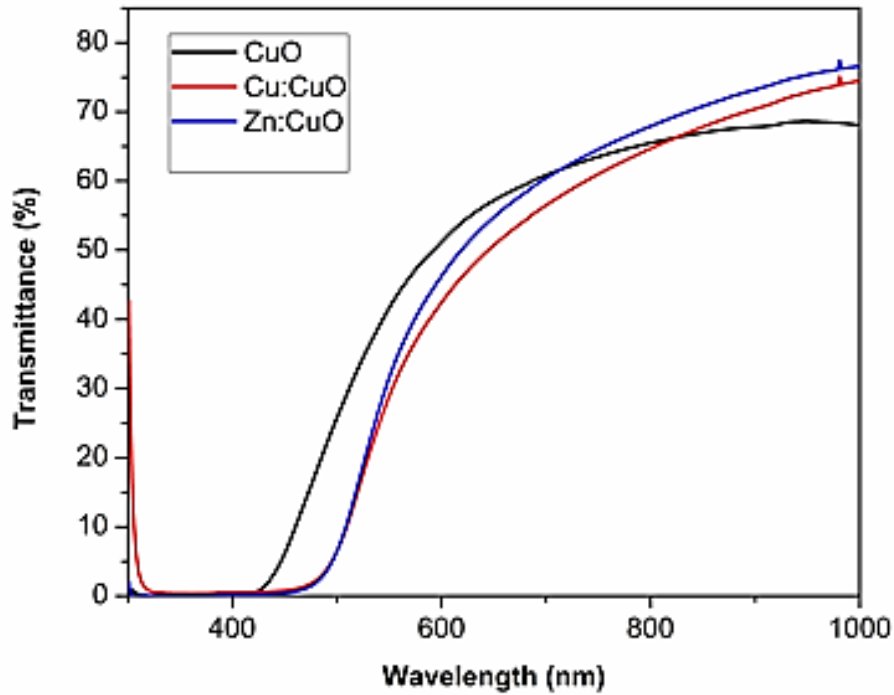


Figure I.17 Optical transmittance of undoped and Cd, Zn doped CuO thin films [16].

Ş. Baturay was studied the morphological and optical properties of a thin film of copper oxide doped Sb with different weight fractions (0, 1, 2 and 3 wt% of Sb). On a soda lime (SLG), glass substrate by spin coating technique. The transmittance of the CuO films changed with an increase in Sb content. Ultraviolet–visible spectrophotometer measurements indicate that a radical increase in the energy band gap of the films with an increase in Sb content from 1.70 to 2.37 eV (figure.I.18) .It can be said that the optical properties of the Sb doped CuO thin film were significantly changed [17].

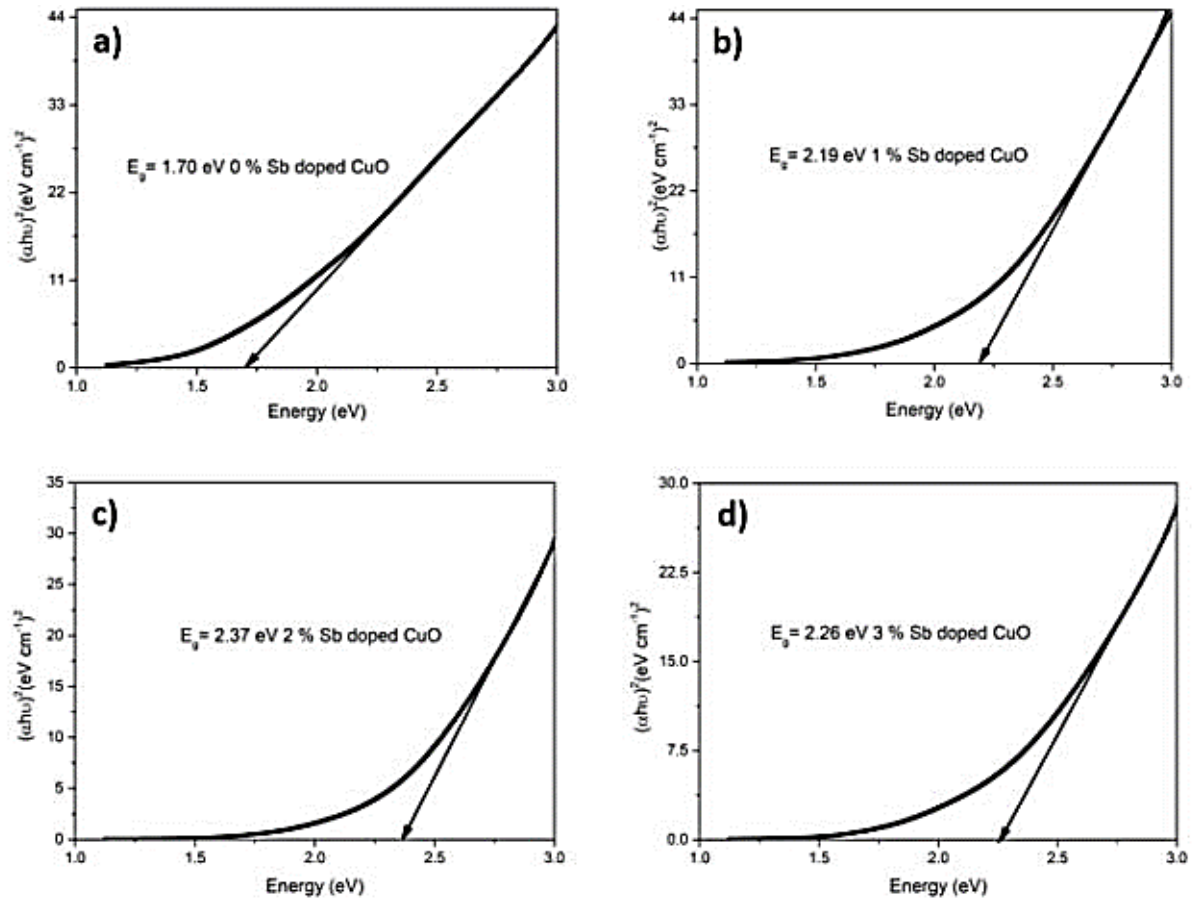


Figure I.18 Energy band gap of a) pure CuO film, b) 1% Sbdoped CuO film, c) 2% Sb-doped CuO film, d) 3% Sb-doped CuO film [17].



References

- [1] M. Lamri Zeggar, «*Cupric Oxide thin films deposition for gas sensor application*», Doctorat thesis, University Freres Mentouri Constantine 1, (2016)
- [2] M. Lamri Zeggar, M.S. Aida, N. Attaf, «*Preparation and characterization of cupric oxide (CuO) thin films deposited by ultrasonic spray pyrolysis*», Journée nationale en Energies Renouvelables and Matériaux Avancés –JNERMA (2018)
- [3] T.H. Tran, V. Tuyen Nguyen, «*Copper Oxide Nanomaterials Prepared by Solution Methods, Some Properties, and Potential Applications: A Brief Review*», International Scholarly Research Notices, (2014).
- [4] P.K.Ooi, S.S. Ng, M.J. Abdullah, H. Abu Hassan, Z. Hassan, «*Effects of oxygen percentage on the growth of copper oxide thin films by reactive radio frequency sputtering*», *Materials Chemistry and Physics*, 140 (2013) 243
- [5] D. S. Murali, S. Kumar, R. J. Choudhary, A. D. Wadikar, M. K. Jain, A. Subrahmanyam, «*Synthesis of Cu₂O from CuO thin films: Optical and electrical properties*» *AIP ADVANCES* 5, (2015) 047143.
- [6] https://www.chemeurope.com/en/encyclopedia/Doping_%28semiconductor%29.html
- [7] <https://www.iue.tuwien.ac.at/phd/wittmann/node7.html>
- [8] <https://www.mrl.ucsb.edu/~seshadri/old/MATRL100A/class12.pdf>
- [9] (<https://www.mrl.ucsb.edu/~seshadri/old/MATRL100A/class12.pdf>)
- [10] A.A. Menazea, A.M. Mostafa, «*Ag doped CuO thin film prepared via Pulsed Laser Deposition for 4-nitrophenol degradation*», *Journal of Environmental Chemical Engineering*, (2020) 1-29.
- [11] H. A. Hussin, R.S. Al-Hasnawy, R. I. Jasim, N. F. Habubi, S. S. Chiad, «*Optical and Structural Properties of Nanostructured CuO Thin Films Doped by Mn*», *Journal of Green Engineering (JGE)*, 10 (2020)1-12.
- [12] H. Z. Asl. S. M. Rozati, «*Spray Deposition of n-type Cobalt-Doped CuO Thin Films: Influence of Cobalt Doping on Structural, Morphological, Electrical, and Optical Properties*», *Journal of ELECTRONIC MATERIALS*, (2019) 1-7.

- [13] A. M. Ahmed, E. Mohamed Abdalla, M. Shaban, «*Simple and Low-Cost Synthesis of Ba-Doped CuO Thin Films for Highly Efficient Solar Generation of Hydrogen*», the Journal of Physical Chemistry C, (2020)1-10.
- [14] A.N. Hussain, M. A. Hassan, K. I. Hassoon, «*Preparation and Characterization of Co Doped Copper Oxide (II) Thin Films by 45° Angle Chemical Spraying Pyrolysis*», Al-Nahrain Journal of Science ANJS, 23 (2020)1-6.
- [15] S. Dinc, B. Şahina, T. Kaya, «*Improved sensing response of nanostructured CuO thin films towards sweat rate monitoring: Effect of Cr doping*», Materials Science in Semiconductor Processing, 105 (2020) 1-8.
- [16] S.J. Helen, R. Chandramohan, «*Influence of Pure and Cd, Zn Doped CuO Thin Films Using Spray Pyrolysis Technique*», Palarch's Journal of Archaeology of Egypt/Egyptology (2020) 1-8.
- [17] S. Baturay, «*Structural and Optical Properties of Sb Doped CuO Films*», Academic Platform Journal of Engineering and Science, (2020) 1-7.

Chapter II:
Metal ions-doped
CuO thin films for
glucose sensors

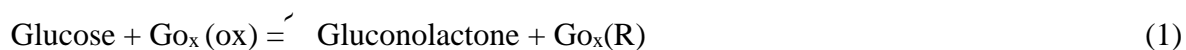
In this chapter, we will introduce several concepts about glucose sensors and their types, followed by a discussion the application of doping CuO in glucose sensors

II.1 Glucose sensors

Diabetes is one of the most common diseases worldwide as it is the leading cause of death and a health problem for most societies. Diabetes mellitus is the most common endocrine disorder of carbohydrate metabolism, and this disease continues to spread and increase [1].

Low blood sugar levels can cause seizures, loss of consciousness, and death in most tissues and organs, including the brain. On the other hand, chronically elevated blood sugar levels can lead to blindness, kidney failure, vascular disease, etc. Neuropathy and therefore the need to keep blood sugar levels within a strict range. The process of keeping blood sugar levels in a steady state is called glucose homeostasis. This is achieved by hormone fine-tuning of glucose uptake during peripheral glucose uptake, hepatic glucose production, and carbohydrate uptake. This is by optimizing a number of parameters, including carbohydrate intake and Intestinal absorption the rate at which peripheral tissues consume glucose and the amount of glucose lost by the kidneys. The body can regulate blood sugar levels through a number of cellular processes in order to avoid high blood sugar levels after eating and low blood sugar levels during fasting. Transport of hormones, cytokines and fuel substrates are important mechanisms of cellular sensing the system [2].

Due to the many applications in the fields of medical diagnosis, management of diabetes, monitoring of vital processes, food industries, and environmental monitoring, more attention has been given to develop a very sensitive and Selective glucose sensors. Diabetes is considered a worldwide metabolic disease. The sensor initiative dates back to 1960s with the revolutionary study of Clark and Lyons, This was followed by the work of the first enzyme-based glucose sensor written by Updike and Hicks 1967. These studies were presented Convincing evidence of how much oxygen is consumed in the glucose-catalyzed glucose oxidase (GOx) reaction oxidation. According to, extensive research has been carried out, studying different types of glucose sensors, including Optical and electrochemical sensors [3].



Glucose, as the most important simple sugar, is a vital characteristic for human health evaluation in clinical medicine. The dynamic monitoring of glucose concentration in the blood is an effective way for diabetes management. According to enzymatic catalytic mechanism, glucose sensor can be divided into enzymatic glucose sensors and non-enzymatic glucose sensors [4].

The concentration of glucose in the blood is a major reason for the health of patients with symptoms of diabetes, so many methods have been followed to measure glucose that have been studied for continuous and accurate monitoring. Electrochemical analysis is a simple and quantitative solution, so this technology has been incorporated into the research level marketing of simple test strips on wearable devices and implantable activities. New methods such as tears saliva, interstitial fluid and sweat are being studied for the determination of blood glucose level. This study includes a review of the development of enzyme-based electrochemical glucose sensors and the development of glucose sensors and integrated devices [5].

Glucose or dextrose, also known as blood sugar, is an energy source for living cells and one of the main products of photosynthesis in prokaryotes and eukaryotes [6].

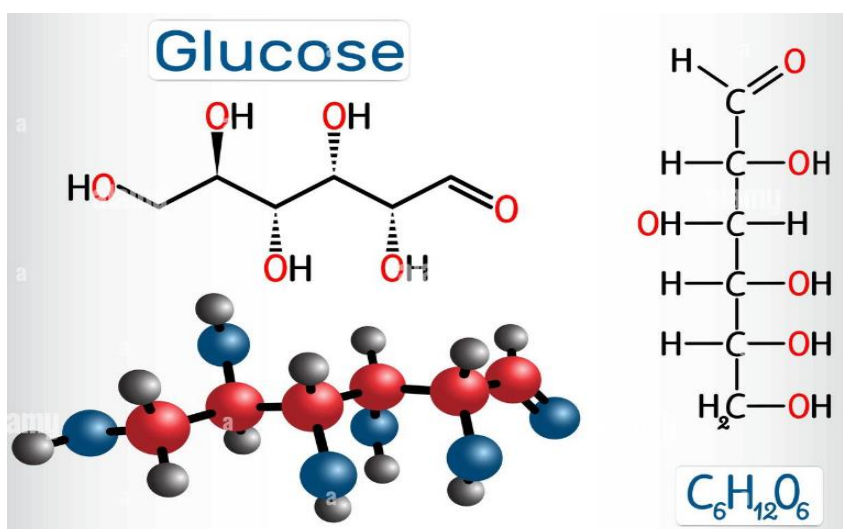


Figure II.1 Structures of glucose [7].

Sensors fall into two categories, passive and active sensors. The passive sensor does not require any additional energy and produces an electrical signal in specific conditions. Among the passive sensors, we find thermal, chemical, thermal and infrared sensors. On the other hand, active sensors, also known as parametric sensors, are used for monitoring from the surface of the atmosphere and meteorology. External active sensors require sources of energy known as an

excitation signal. Because of their special characteristics in reaction to an external stimulus, they are converted into electrical signals [8].

Table II.1 Sensors based on their detection properties [8].

Types	Properties
Thermal sensor	Temperature, heat, flow of heat...
Electrical sensor	Resistance, current, voltage, inductance, etc.
Magnetic sensor	Magnetic flux density, magnetic moment, etc.
Optical sensor	Intensity of light, wavelength, etc.
Chemical sensor	Composition, pH, concentration, etc.
Pressure sensor	Pressure, force, etc.
Vibration sensor	Displacement, acceleration, velocity, etc.
Rain/moisture sensor	Water, moisture, etc.
Tilt sensors	Angle of inclination, etc.
Speed sensor	Velocity, distance, etc.

II.1.1.Type of glucose sensors

Electrochemical sensors are generally divided into two categories, enzymatic and non-enzymatic glucose sensors.

II.1.1.1. Enzymatic glucose sensors

Enzyme-based sensing is used to know blood glucose levels and is the most popular method, due to its high sensitivity and selectivity for glucose. Glucose is oxidized in the presence of the (Gox) enzyme, which is widely used by many glucose sensors. In addition, these enzymes are subject to a large variety of environmental conditions such as temperature and pH during the measurements, due to their inherent nature. To reduce the activity of this enzyme, it is immobilized on rigid interfaces obtained through various strategies such as physical adsorption, covalent bonding and.... The sensitivity of the glucose sensor is determined by the activity of immobilized enzymes [3].

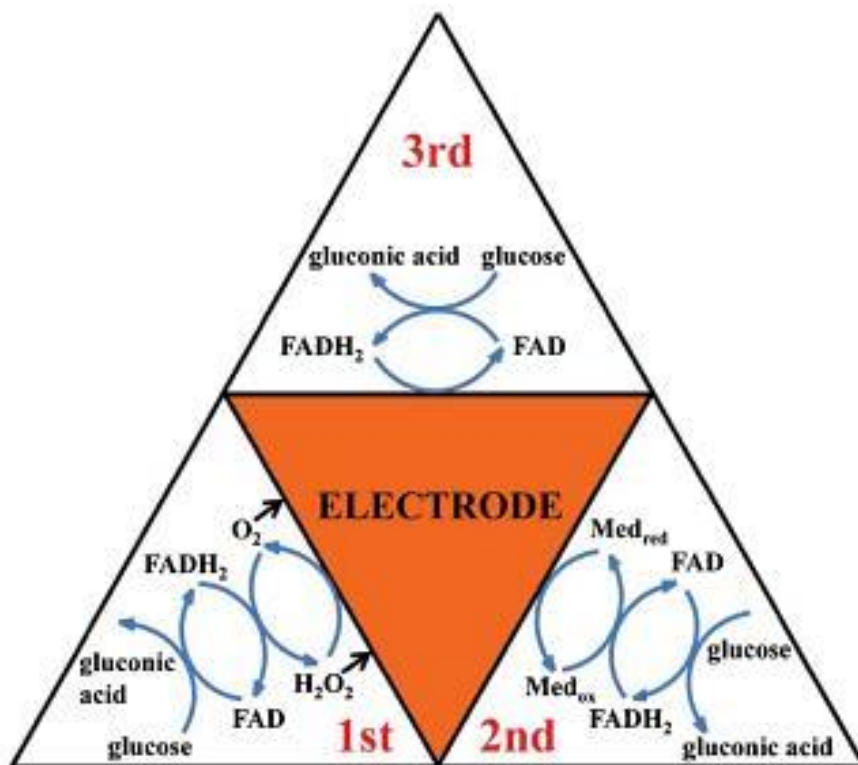


Figure II.2 Summary of enzymatic glucose oxidation mechanisms, presented as first, second, and third [3].

a) Working principle of enzymatic glucose sensors

Enzyme electrodes, usually composed of substrate electrodes, substrates materials, glucose oxidase and nafion ion exchange membrane, are the most important part of these types of glucose sensors. Most of the current research on glucose sensors focus on improving their response to glucose, i.e. more electrons should be in the enzyme electrode is then efficiently captured by the substrate electrode. Exist On the one hand, the electron yield is limited by the amount of GOx adsorption on the substrate the material is controlled by the surface of the base material. On the other hand, the transport rate of these electrons depends on the conductivity of the matrix material. The result is it is important to find the optimal matrix material for immobilization of glucose oxidase (GOx). Improving the performance of enzymatic glucose sensors [9].

Glucose oxidase produces an oxidative current monitored by an electrochemical glucose biosensor. Free glucose is catalyzed by Gox and produces gluconic acid and hydrogen peroxide (H₂O₂). The H₂O₂ produced by GOx is deprotonated to generate free protons, which dissolve oxygen and 2 electrons at an external oxidation potential. The detected electrical signal is proportional to the glucose concentration [10].

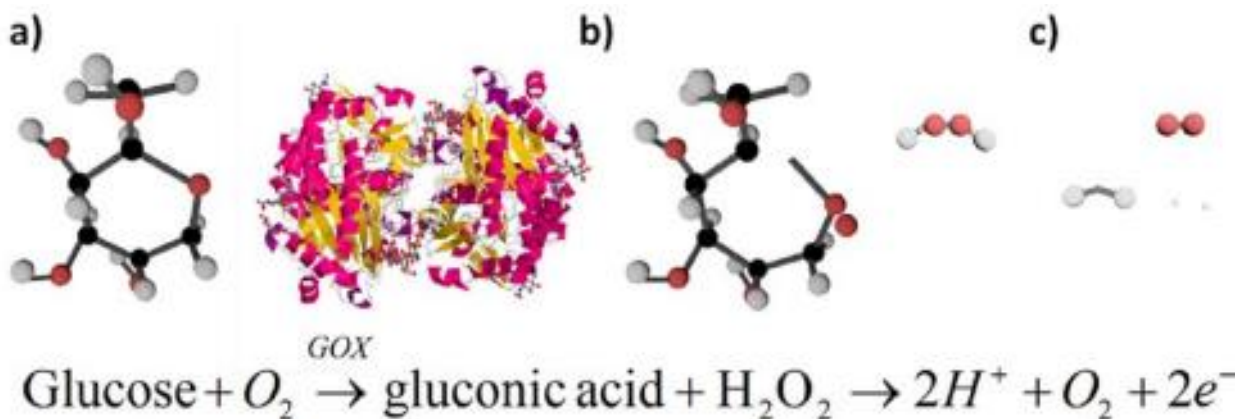


Figure II.3 Basic working principle for glucose biosensors, a) Glucose binds in the enzymatic binding pocket of glucose oxidase, b) An applied potential catalyzes the oxidation of glucose to gluconic acid and hydrogen peroxide, c) Hydrogen peroxide dissociates to O_2 , $2H^+$, and $2e^-$. [10]

II.1.2.2 Non-enzymatic glucose sensors

This sensor has high sensitivity because it uses direct electro-catalytic oxidation of Glucose on electrode surface, long-term stability, resistance to temperature effects, low Response time and repeatable manufacturing. To make a non-enzymatic glucose sensor, various materials have been used, such as noble metals (Au, Pt, etc.), transition metals, Metal alloys, conducting polymers, graphene and metal oxides [11].

a) Working principle of non-enzymatic glucose sensors.

Most non-enzymatic glucose sensor electro-catalysts have catalytic effects associated with the metal centers of the materials. There are now two widely accepted theories to explain this Catalytic process of glucose on the electrode surface. Adsorption of active chemicals by electrode materials is used in a variety of electro catalytic processes. Pletcher originally developed a chemisorption model for glucose oxidation, in which the d orbitals of metal atoms are bound to glucose molecules. The catalytic process is shown in the figure below:

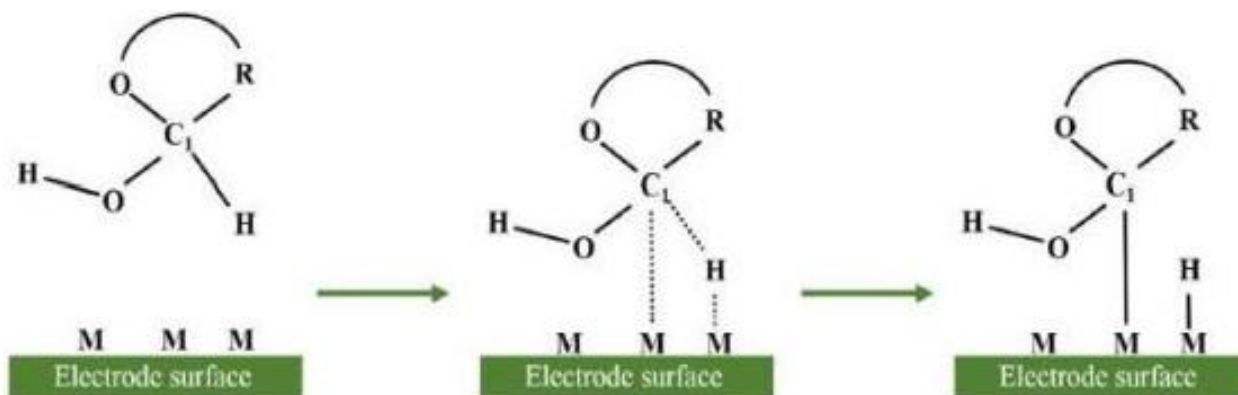


Figure II.4 An illustration of the chemisorption model in glucose oxidation. M: metal atom; C1: hemiacetalic carbon atom; R: other parts of the glucose molecule [12].

Under the action of the electrode, the C1 atom of glucose and the hemiacetal hydrogen atom is cleaved. This dehydration and Chemisorption of glucose, a key step in controlling the rate of the reaction. That adsorb ate is oxidized to gluconolactone, which is then converted to gluconic acid electrode surface. Since the adsorbent occupies the catalytic center of the electrode Materials that alter the nanostructure and morphology of catalysts to improve active sites the material can increase the rate of glucose oxidation [12].

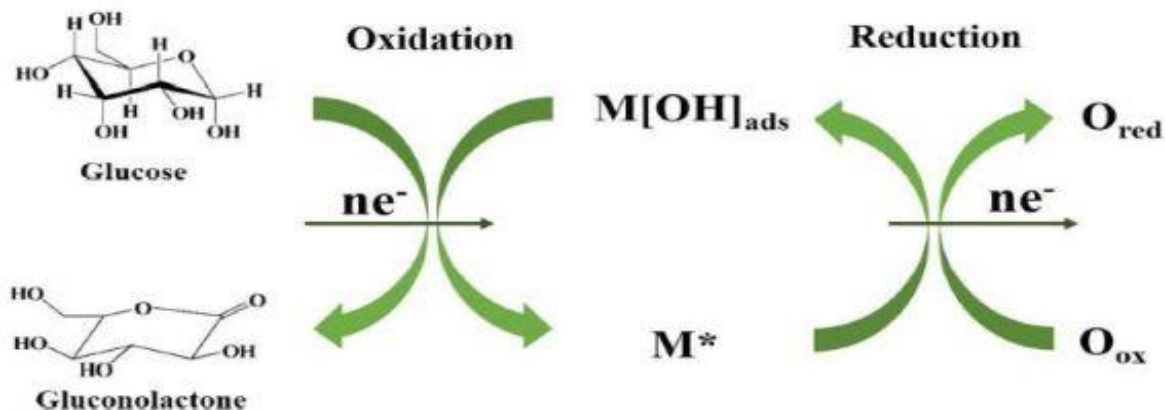


Figure II.5 The schematic diagram of incipient hydrous oxide adatom mediator model. M* is the reductive metal adsorption site. M [OH] ads stands for oxidative adsorbed hydroxide radical [12].

The metal oxides on the electrodes are oxidized by the bias of the anode. The formed oxides with higher oxidation numbers have strong oxidative power and can form surface-bound OH_{ads} radicals, which play a crucial role in the glucose catalysis process. To improve the formation of OH_{ads}, the electro-oxidation of glucose is usually carried out in alkaline solution, which can also ensure the durability of metal oxide-based electrodes [12].

II.2 Application of doping CuO in glucose sensors

The concentration of glucose in human blood can have a worrying effect on human health, so the distribution of blood glucose impurities in the human body is an important indicator that can be used to monitor diabetes. Diabetes affects many parts of the body such as B. nerve damage, erectile dysfunction and arteriosclerosis leading to organ loss [13].

In this study, C. Cheng et al. [13] used a periodic voltmeter (CV) to manipulate the electrical properties of the solution by preparing electrodes with CuO nanoparticles modified with tetragonal ZnO nanostructures deposited on fluorinated tin oxide glass (CuO/ZnO/FTO). The schematic illustration of the synthesis of a non-enzymatic glucose sensor electrode is shown in figure II.6.

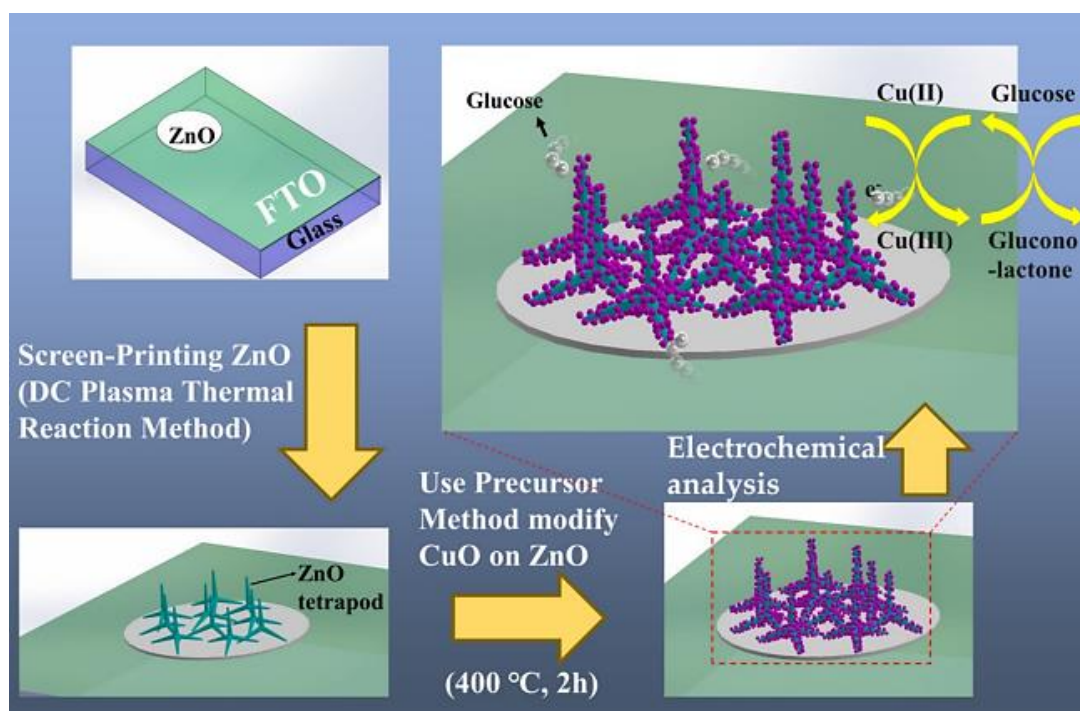


Figure II.6 Schematic illustration of the synthesis of a non-enzymatic glucose sensor electrode [13].

Measurements were processed in glucose solutions of different concentrations with the aim of developing sensor sensitivity. Different immersion times in the copper sulfate solution precursor were also used to prepare the electrode and conduct electrochemical studies to adjust the electrode capacity. The modified electrode, which was immersed in copper sulfate for 30 s, was effective in detecting glucose molecules at different concentrations at a voltage of +0.6 V. The upward slope is closely and positively correlated with glucose concentration. One important result is to indicate

that the glucose concentration is linearly proportional to the present value of the CV (Figure.II.7) [13].

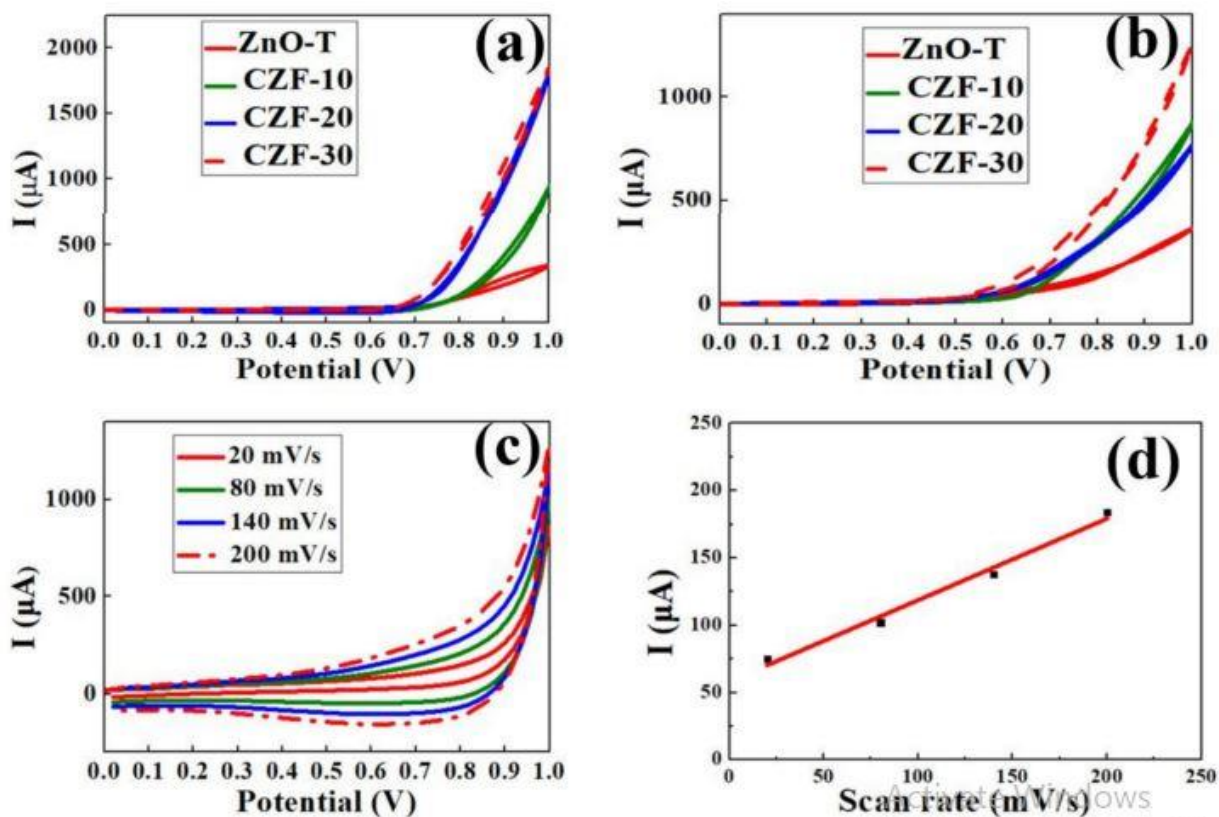


Figure II.7 (a) CVs of different electrodes at a scan rate of 100 mV/s in 0.1 M NaOH (b) CVs of different electrodes at a scan rate of 100 mV/s in 0.1 M NaOH add 0.1 mM glucose. (c) CVs of the CZF-30 in 0.1 M NaOH containing 1 mM glucose at different scan rates from 20 to 200 mV/s. (d) shows the anodic peak current vs. scan rate [13].

After the measurement test with the addition of interference, the sensor can still determine the concentration of glucose in the solution unaffected. This result proves that the sensor has great potential to develop into a high-performance non-enzymatic glucose sensor [13].

At the same time, another work is carried out by M. Palmer et al., they presents a dataset of plasma-enhanced nitrogen doping of oxide-free CuO-NiO in hybrid films in a short paper. CuO, NCuO/Cu₂O, CuO: NiO and N-CuO/Cu₂O: NiO were compared. The produced films are used in glucose sensor applications. Nitrogen dopant species generated during plasma ignition lead to a favorable phase shift from CuO to Cu₂O. Several characterization techniques are used to study the morphology, structural characteristics, doping appearance, and electrical properties of the various electrodes developed [14].

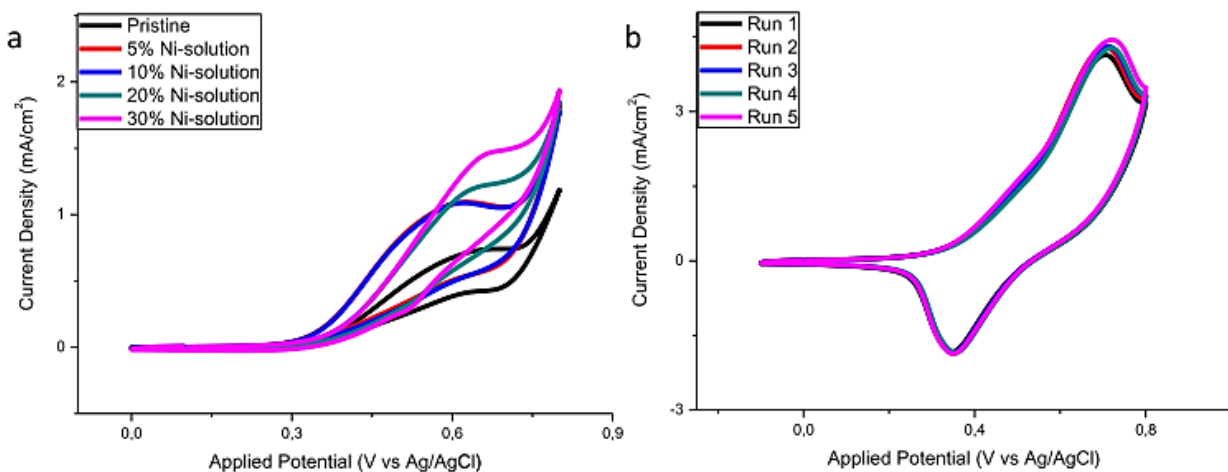


Figure II. 8 CV diagrams conducted at a scan rate of 25 mV/s for (a) comparison of the effects of Ni solution on the peak oxidation current and (b) repeatability of N-CuO/Cu₂O: NiO sensor in 1 mM glucose solution [14].

The electrochemical performance of the thin film sensor was tested using cyclic voltammetry and time measurement (figure II.9). CuO has a sensitivity of 830 $\mu\text{A}/\text{mM}\cdot\text{cm}^2$ for 1.65 mM glucose; N-CuO/Cu₂O has a linear range of up to 1.91 mM and a sensitivity of 873 $\mu\text{A}/\text{mM}\cdot\text{cm}^2$, and CuO: NiO electrodes have a linear range of up to 1.65 mM and a sensitivity of 1103 $\mu\text{A}/\text{mM}\cdot\text{cm}^2$ [14].

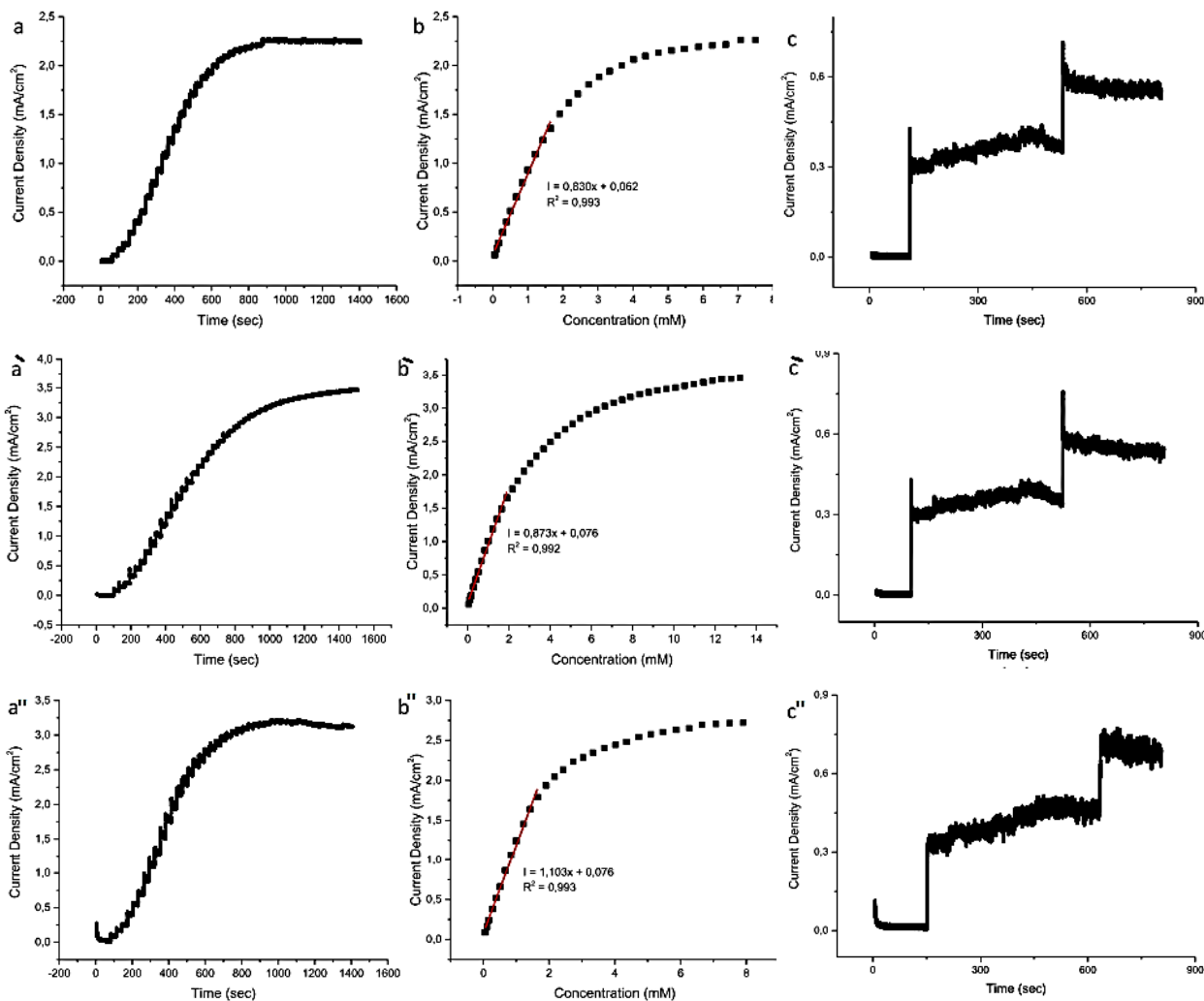


Figure II.9 Amperometric response of: N-CuO/Cu₂O, CuO: NiO and CuO: NiO sensor to a, a' and a'') successive additions of glucose, b, b' and b'') corresponding calibration curve including the linear range and c, c' and c'') interference species of biological samples, respectively [14].

On the other hand, R. Ahmad et al. [15] developed vertically aligned ZnO nanosticks (NRs) on perfluorinated tin oxide (FTO) electrodes and decorated with CuO to achieve a high-performance of non-enzymatic glucose sensor. This unique combination of CuO-ZnO-NRs has a high surface area and structure that easily penetrates the substrate, resulting in improved electrochemical performance of glucose oxidation.

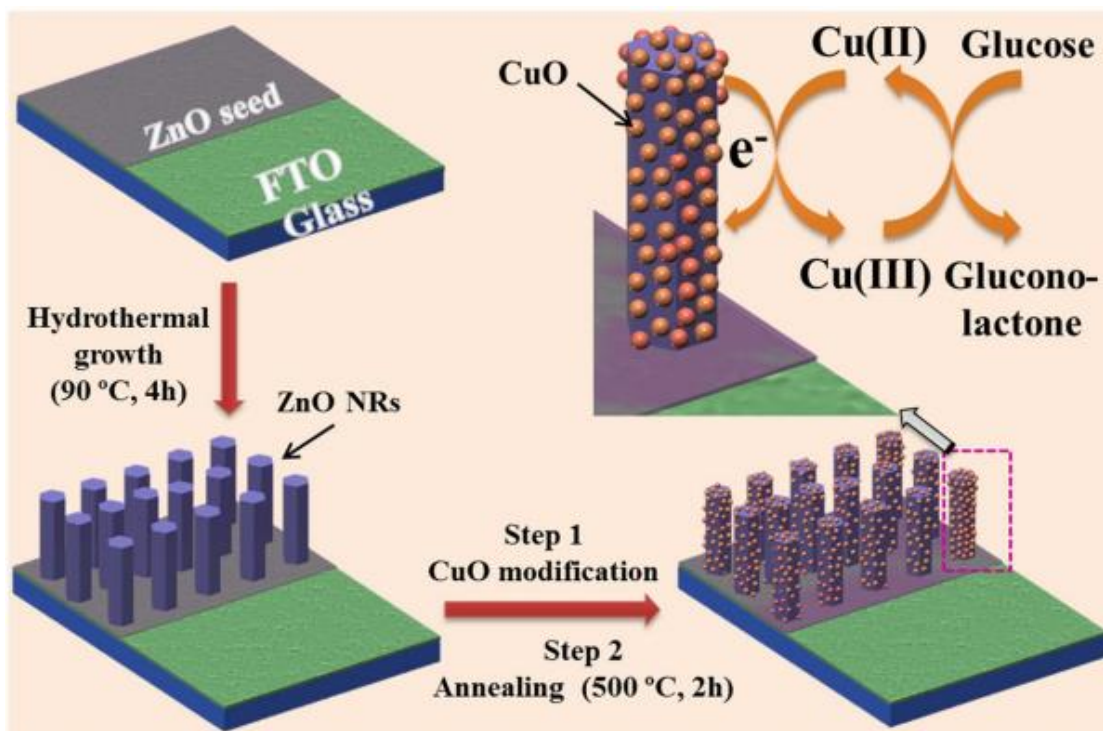


Figure II.10 Schematic diagram of the fabrication of the non-enzymatic glucose sensor electrode and its application in glucose detection [15].

As a result, the electrodes have a high sensitivity ($2961.7 \mu\text{A mM}^{-1} \text{cm}^{-2}$), a linear range of 8.45 mM, a low limit of detection ($0.40 \mu\text{M}$), a fast response time (2 s), as well as excellent reproducibility. Repeatability, stability, selectivity and applicability of glucose detection in human serum samples. To circumvent this issue, CuO-modified ZnO NRs show excellent performance as an efficient electro-catalyst for glucose detection and also provide a new prospect for biomolecules synthesized by the detectors [15].

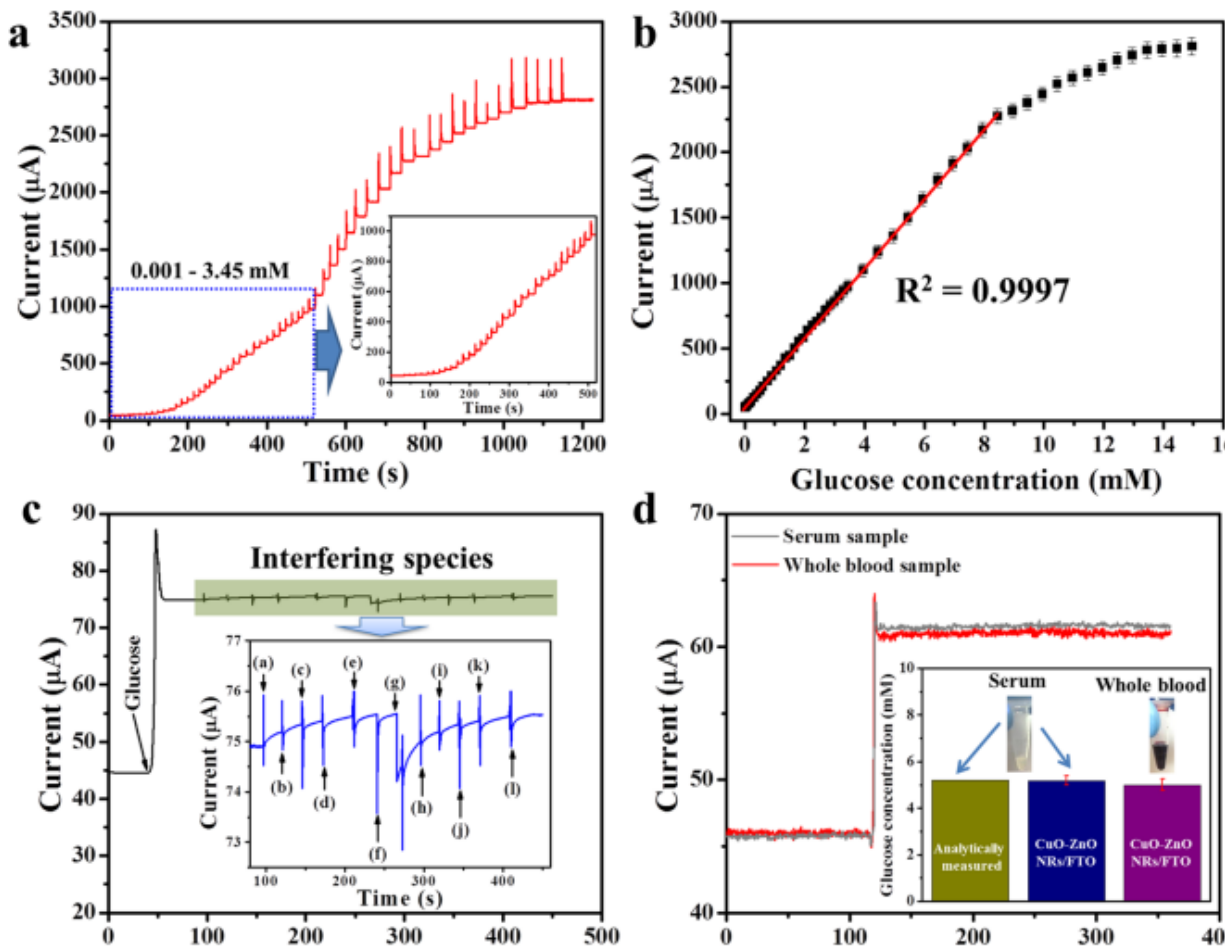


Figure II.11 Non-enzymatic detection of glucose. (a) Amperometric response of CuO-ZnO NRs/FTO electrode at +0.62V/Ag/AgCl in 0.1M NaOH solution with different glucose concentration (b) Corresponding calibration plot of current response versus glucose concentration. (c) Anti-interference ability test. Amperometric response of the CuO-ZnO NRs/FTO electrode with the addition of 0.1mM glucose and 0.02Mm of each possible interfering species i.e. (a) AA, (b) UA, (c) DA, (d) NADH, (e) Mg^{2+} , (f) Ca^{2+} , (g) Cys, (h) NaCl, (i) lactose, (j) sucrose, (k) maltose, and (l) mannose in the 0.1M NaOH solution at +0.62V (versus Ag/AgCl). (d) Real sample glucose detection. Amperometric response of CuO-ZnO NRs/FTO electrode at +0.62V/Ag/AgCl in 9.5mL 0.1M NaOH solution after injecting 0.5mL blood serum (i) and freshly drawn whole human blood (ii). The upper inset shows the photograph of serum and whole blood samples and lower inset shows the histogram of glucose concentration compared with blood chemistry analyzer result [15].

In addition, A. Senthamizhan et al. [3] Developed nanofiber glucose sensors using different fibres. Our in-depth analysis included greater performance for electrically spun nanofiber sensors compared to sensors based on nanomaterials, although they are highly active. In particular, electrospun nanofibers have properties that make them a good choice for sensor applications including their high surface area, porosity, flexibility, cost-effectiveness, and portable nature. Thus, electrospun nanofiber-based glucose sensors offer a number of advantages, including increased shelf life, which is highly essential for practical applications.

Figure II.12 (a-e) shows the fabrication process of PEDOT with built-in GOx on a microelectrode array. The method involves the electrolytic deposition of GOx-infused PEDOT thin films (PEDOT F-GOx) on the surface of platinum (Pt) microelectrode arrays. Then, poly (L-lactide) (PLLA) nanofibers were fabricated directly on Pt microelectrode arrays to obtain GOx-incorporated PEDOT nanofibers (PEDOT NFs-GOx). To obtain GOx-incorporated PEDOT nanofibers (PEDOT NFs-GOx), poly (L-lactide) (PLLA) nanofibers were first electrospun directly onto Pt microelectrode arrays. Subsequently, electrochemical deposition of PEDOT was performed on the Pt microelectrodes and around the PLLA nanofibers in a manner similar to that of PEDOT F-GOx. Figure II.12 (h-m) shows the optical and SEM images of Pt microelectrode arrays, PEDOT F-GOx, and PEDOT NFs-GOx on Pt sites. The authors highlight four advantages of the designed sensor, namely the presence of a nanoscale matrix for GOx entrapment, reduced impedance, increased GOx entrapment in PEDOT, and glucose detection at lower potentials [3].

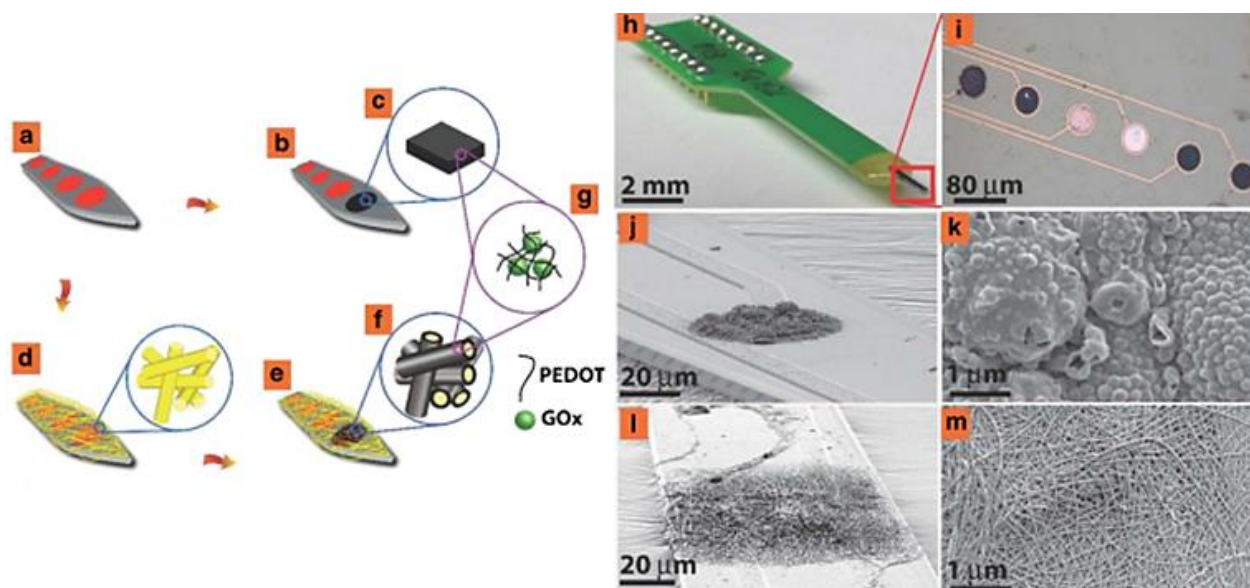


Figure.II.12. Schematic of fabrication process of GOx-incorporated PEDOT on the microelectrode array: (a) Pt microelectrode array. (b), (c) Electrodeposition of GOx incorporated PEDOT film. (c) Electrospinning of PLLA nanofibers on the microelectrode array. (d), (f) Electrodeposition of PEDOT around the PLLA nanofibers to form GOx incorporated PEDOT nanofibers. (g) Schematic of entrapment of GOx within PEDOT structure. (h) Optical micrograph of entire microelectrode array. (i) Optical micrograph of microfabricated electrode. (j) SEM of PEDOT F-GOx. (k) Higher magnification SEM of PEDOT FGOx. (l) SEM of PEDOT NFs-GOx. (m) Higher magnification SEM of PEDOT NFs-GOx [3].

Subsequently, the electrochemical performance of metal oxide nanofibers was enhanced by incorporating various metals and nanoparticles. Zinc oxide (ZnO) nanofibers are considered to be one of the best-known materials with remarkable properties in terms of biocompatibility, nontoxicity, stability, and electrochemical activity. A three-dimensional network was devised by Zhou, C. et al. Composed of layered 1D ZnO-CuO nanocomposites (HNCs) and investigated their enzyme-free sensing properties by varying the thickness of the 3D network in the glucose direction. Pure CuO NWs and mixed ZnO/CuO NWs were also prepared by electrospinning for comparative studies. The results of the reaction of the non-enzymatic process to glucose are shown in Figure II.13. Due to lower economic benefits, higher sensitivity, lower detection limits and faster response times, a huge need to reduce sensors to the level of individual probes has been observed.

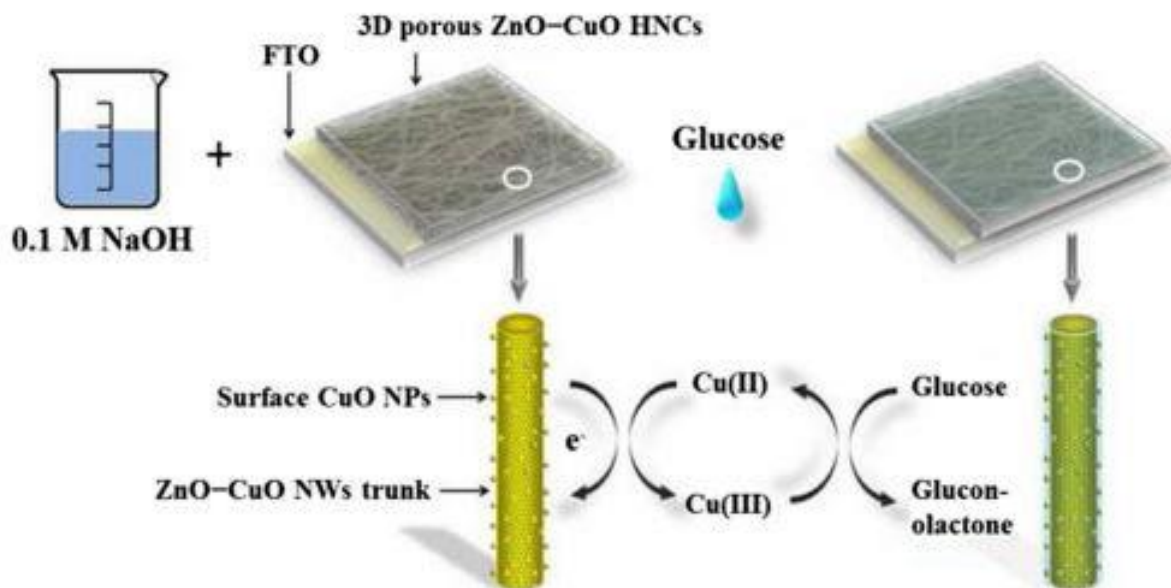


Figure II.13 Reaction mechanism of 3D porous ZnO–CuO HNCs electrodes [3]

In addition, this research has been devoted to improving cognitive performance by exploiting the synergistic effects of the two components. The immobilization of metal nanoparticles on metal oxide nanofibers was observed to increase the sensitivity of the sensor. Zheng, B. et al. report the fabrication of copper oxide nanofibers (Ag/CuO NFs) decorated with silver nanoparticles for non-enzymatic glucose sensors. Figure II.14 schematically depicts the fabrication process of Ag/CuO NFs on ITO electrodes. Interestingly, the response time was found to be faster than the enzyme-based glucose sensor because the electrospun NFs were directly deposited on the ITO electrode surface.

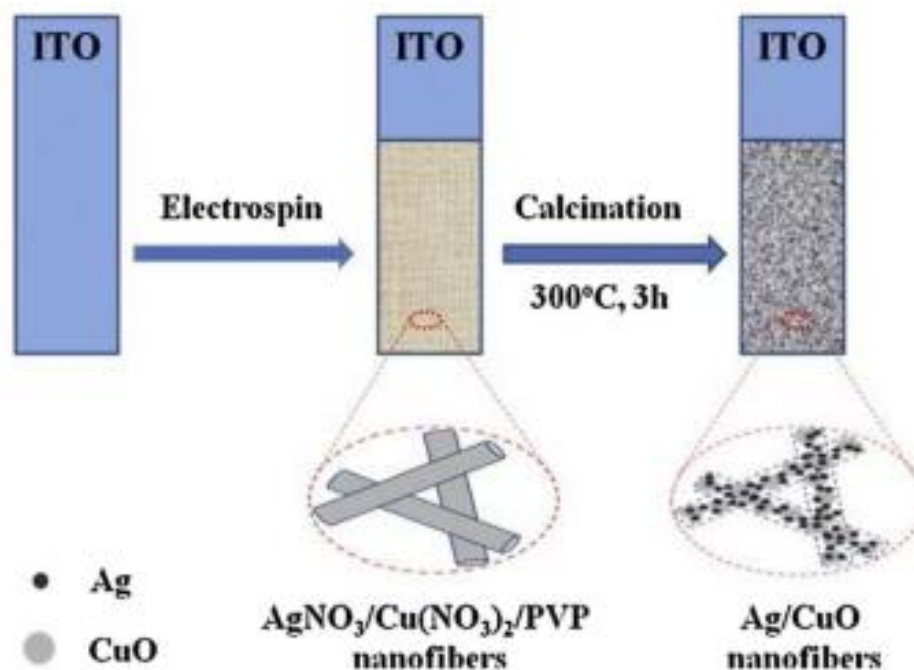


Figure II.14 The preparation process of Ag/CuO NFs-ITO electrode. [3]

Although the linear operating range is narrow, as shown in Figure II.15.d, Ag/CuO-NFs-ITO is about 2.4 times more sensitive to glucose than CuO-NFs-ITO at 0.50 V. The obtained results highlight the enhancement of sensor sensitivity by incorporating AgNPs into CuO NFs. The underlying reason for this mechanism is that AgNPs not only enhanced the electron transfer between the Ag/CuO hybrid NFs and the ITO electrode, but also enhanced the electron transfer between the Ag/CuO NFs and the glucose molecules present in the solution. Recent reports have demonstrated that well-defined porous nanostructures prove to be ideal electrode materials for glucose oxidation due to their large surface area, high porosity, and open geometry, which facilitates the electrolyte interaction at the electrode-electrolyte interface Mass and Electronic Transmission [3].

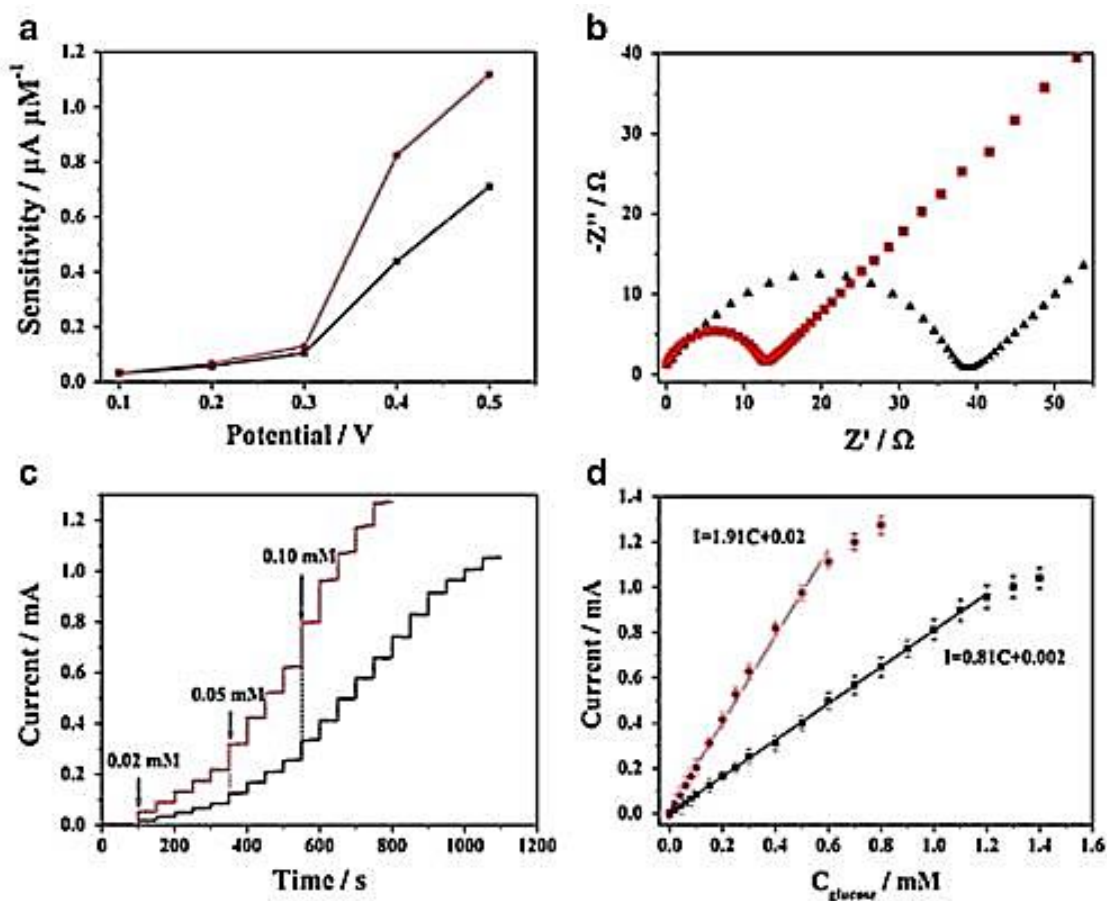


Figure II.15 a) Effect of applied potential on the sensitivity of Ag/ CuO NFs–ITO (Red) and CuO NFs– ITO (black) electrodes to glucose. b) Nyquist plots of Ag/CuO NFs– ITO and CuO NFs–ITO electrodes in 0.10 M KCl solution containing 5.0 mM $[\text{Fe}(\text{CN})_6]^{3- / 4-}$ redox couple. c) Amperometric response of Ag/CuO NFs– ITO and CuO NFs–ITO to successive additions of glucose at an applied potential of 0.50 V. d) Calibration curves obtained from (C) [3].

On the other side, X. Wang et al. [4] has developed an ultra-sensitive and highly stable non-enzymatic glucose sensor with CuO nanostructures through a simple and low-cost wet chemical pathway. Three types of CuO nanostructures were obtained by kinetic control.

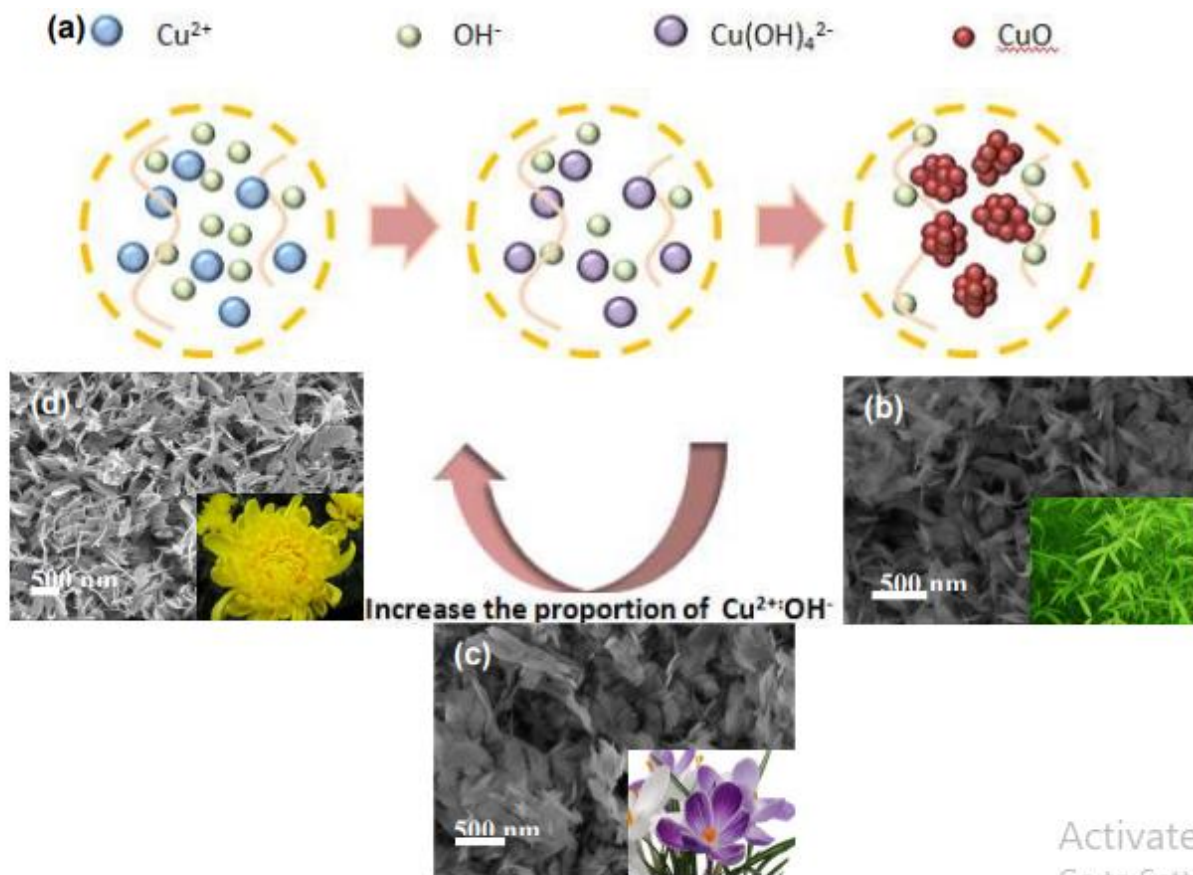


Figure II.16 (a) Schematic illustration of CuO nanostructures evolution; SEM images of CuO ultrafine power with the ratio $\text{Cu}^{2+}:\text{OH}^- = 1:5$ (b); $1:8$ (c); and $1:10$ (d) [4].

The best freshly made CuO electrode with a rough petal-like structure has a high quantum sensitivity of $7546.37 \mu\text{A cm}^{-2} \text{mM}^{-1}$ and an extremely low detection limit of $0.259 \mu\text{M}$, much better than some previous reports. In the alkaline environment, the rough petals can increase the dynamic contact area for mass transfer between the CuO nanostructures and the electrodes, thus significantly improving the electrooxidation performance of glucose. In addition, the non-enzymatic glucose sensor prepared as such showed excellent anti-interference performance, fast response time, good reproducibility and long-term stability. Therefore, the synthetic CuO electrode could be a promising material for non-enzymatic glucose sensor applications.

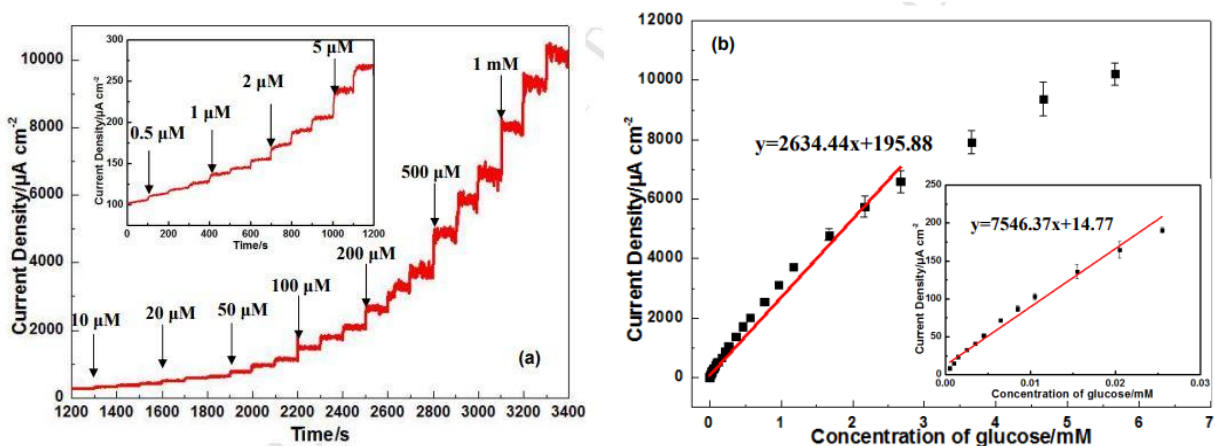


Figure II.17 Amperometric response of Nafion/CuO8/GCE and controls to interfering species (a) and sugars (b) at representative physiological concentration levels, respectively [4].

F. Cao et al. [16] has fabricated an improved non-enzymatic glucose sensor based on nickel oxide-saturated copper oxide microfibers (CuO-NiO-MFs) on fluorine tin oxide (FTO) electrodes by electrospinning and sintering techniques. Cyclic voltammetry (CV) and temporal voltammetry results show that the electro-catalytic activity of the glucose-modified CuO-NiO MFs electrodes is much higher than that of the nickel oxide-modified electrodes (NiO MFs).

The lowest detection limit (signal/noise ratio (S/N) = 3) of a non-enzymatic glucose sensor based on CuO-NiO MFs was 1×10^{-9} M with a highest sensitivity of $3165.53 \mu\text{A mM}^{-1} \text{cm}^{-2}$. Moreover, it was used to detect glucose concentrations in human serum samples in good agreement with the results of automated biochemical analyzers [16].

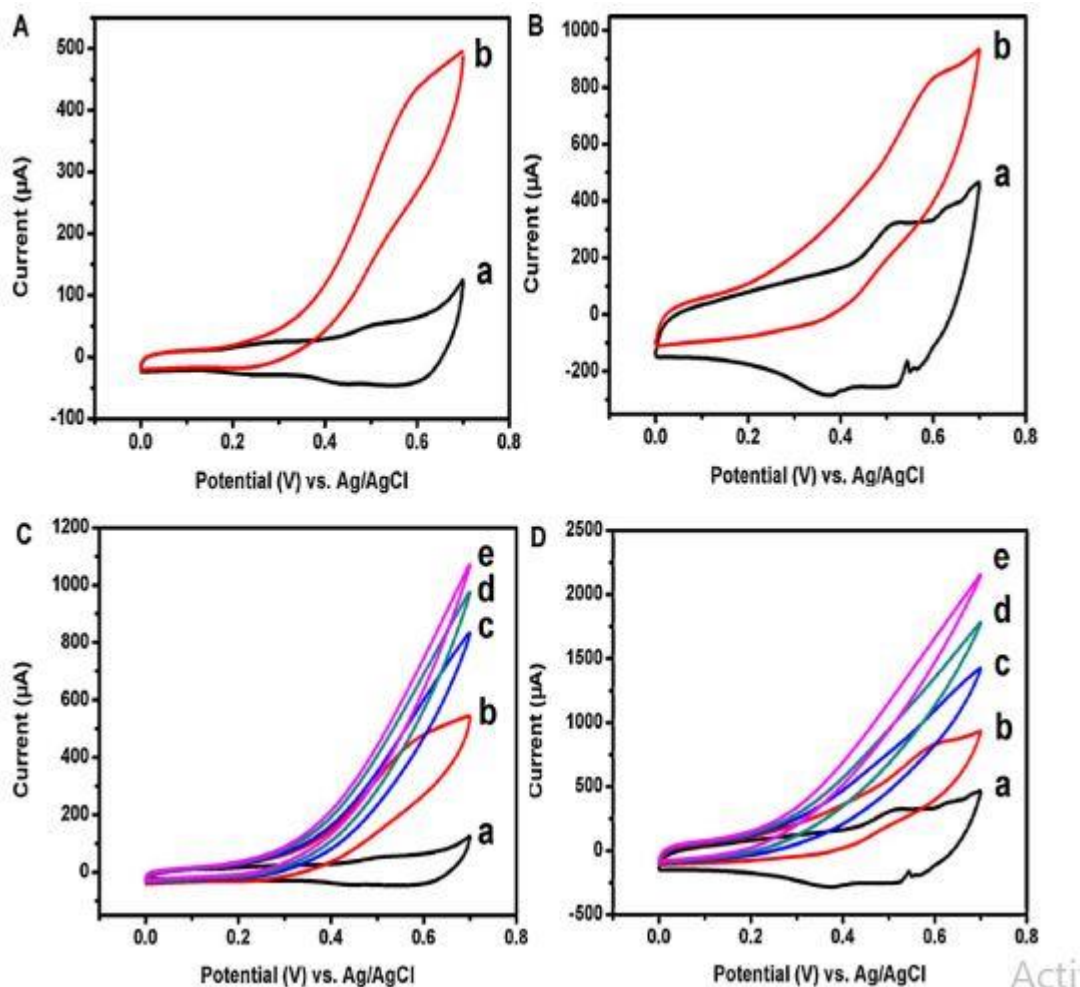


Figure II.18 (A) CVs of the NiO-MFs modified electrode in the (a) absence and (b) presence 1 mM of glucose in 0.1 M of NaOH; (B) CVs of the CuO-NiO-MFs modified electrode in (a) absence and (b) presence 1 mM of glucose in 0.1 M of NaOH; (C, D) CVs of the NiO-MFs and CuO-NiO-MFs modified electrode, respectively, in 0.1 M of NaOH with (a) 1, (b) 2, (c) 3, and (d) 4 mM of glucose, scan rate fixed at 50 mVs^{-1} [16].

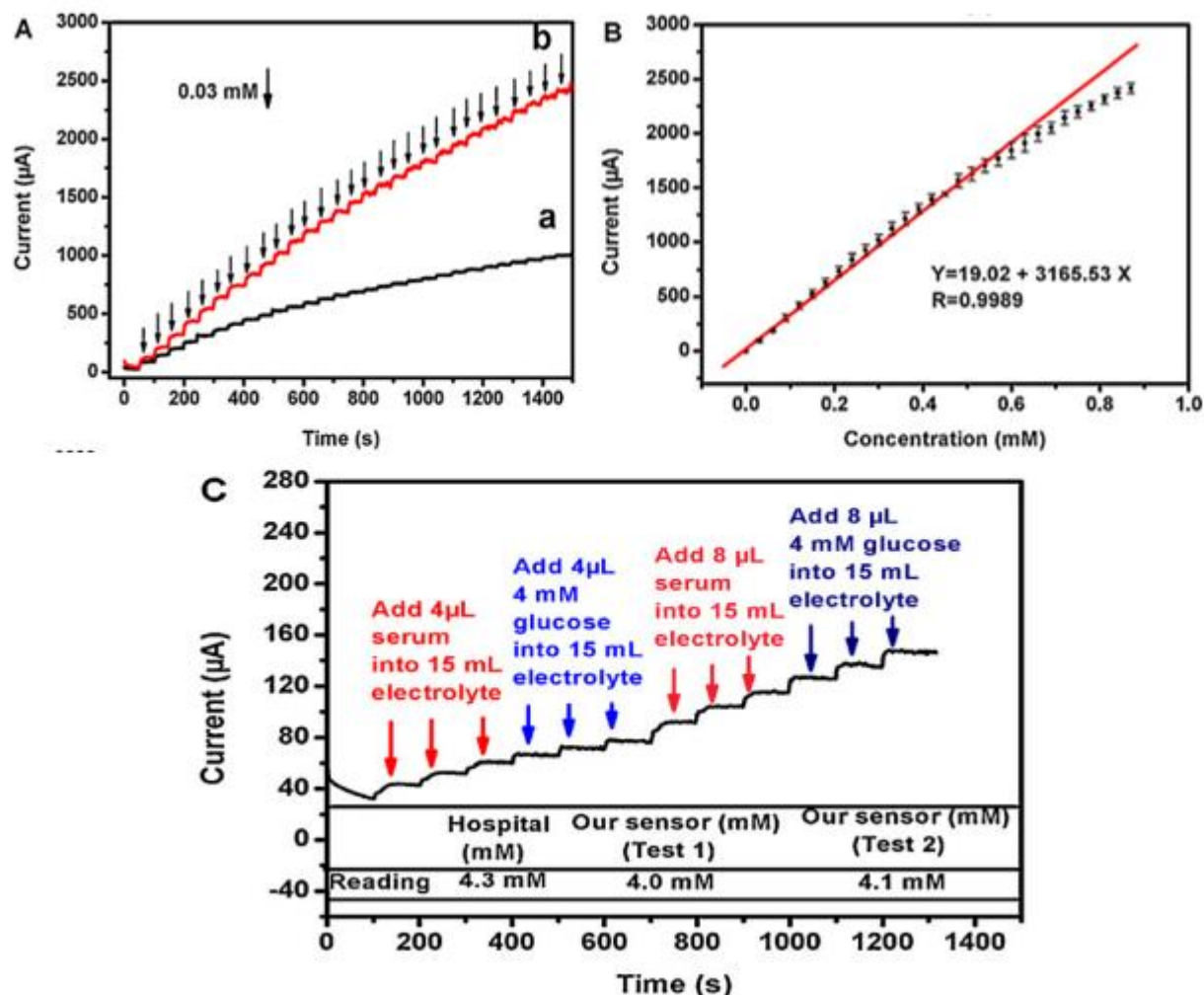


Figure II.19 (A) Amperometric response of (a) the NiO-MFs and (b) the CuO-NiO-MFs modified electrode upon successive addition of glucose at 0.03 mM to 0.1 M of NaOH at an applied potential of 0.5V; (B) the calibration curve for the amperometric response of the CuO-NiO-MFs modified electrode;(C) amperometric response of the CuO-NiO-MFs modified electrode with successive 3-time addition of analytes in the sequence of 4 μL of blood serum sample, 4 μL 4 mM of glucose, 8 μL of blood serum sample and 8 μL 4 mM of glucose in 0.1 M of NaOH solution [16].

AA and DA are the main interferences that usually occur with glucose in real samples (human blood). Comparing the current response of each interferent at the same concentration is an easier way to demonstrate sensor selectivity. Figure II.20.A shows the amperometric response of four consecutive repeated additions of interferences in the order of 0.3 M DA, 0.3 M AA, 0.3 M glucose, and 3 M glucose in 0.1 M NaOH solution. This study showed that the current response produced

by glucose was much higher than that of DA or AA at the same concentration (0.3 M), indicating good selectivity for glucose [16].

The stability of the CuO-NiO-MFs modified electrode was evaluated by measuring its current response to 2 mM glucose over 15 days (Figure.II.20.B). The electrodes decorated with CuO-NiO-MFs were exposed to air and their current performance was tested daily. The sensor based on CuO-NiO MFs showed good stability, losing only about 18% of the current response after 15 days. Therefore, CuO-NiO MFs are good electrode materials for fabricating sensitive, stable and reproducible current sensors for glucose determination [16].

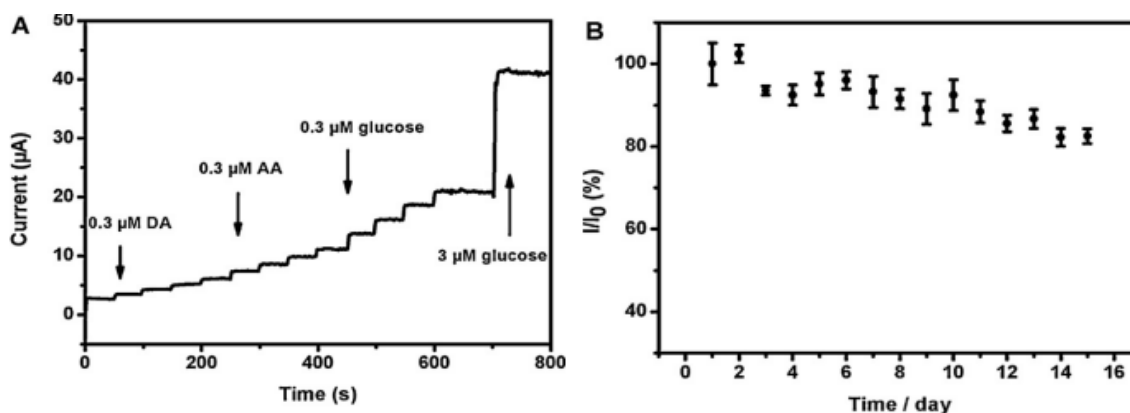


Figure II.20 (A) Amperometric response of the CuO-NiO-MFs modified electrode with successive 4-time additions of interferences in the sequence of 0.3 M of DA, 0.3 M of AA, 0.3 M of glucose and 3 M of glucose in 0.1 M of NaOH solution; (B) stability of the CuO-NiO-MFs modified electrode stored at ambient conditions over 15-day periods in the presence 2 mM of glucose in 0.1 M of NaOH solution. [16].

In 2009, W. Wang et al. [17] successfully synthesized CuO nanofibers (PCNFs) by electrospinning, and then used them to construct the current non-enzymatic glucose sensor. Glucose sensors based on PCNFs display clearly enhanced electro-catalytic activity toward glucose oxidation. In addition, excellent selectivity, reproducibility and stability were obtained. These results indicate that PCNFs are promising candidates for non-enzymatic glucose detection by tonometry.

Figure II.21.a presented the XRD patterns of pure CuO nanofibers and PCNFs. A distinct monoclinic structure of CuO was detected in both samples and there is no indication that any dopant-related phase exists in the Pd-doped samples due to high dispersion or poor crystallinity of the dopant-related nanoparticles. To demonstrate the presence of Pd components in PCNFs, XPS

was used to study the binding properties and oxidation states of Pd in the assembled nanofibers. As shown in Figure II.21.b, the Pd 3d spectrum shows two peaks centered at 337.4 eV and 342.6 eV, respectively, indicating the presence of the Pd component and the binding state of palladium confirming the Pd⁴⁺[17].

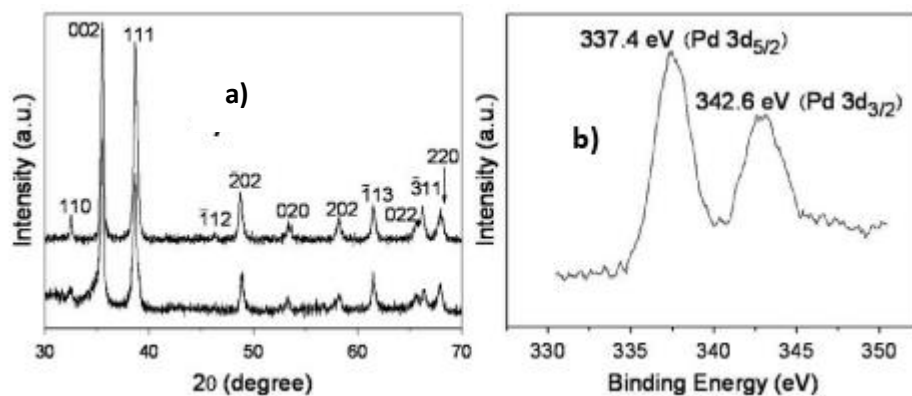


Figure II.21 a) XRD patterns of the products and b) XPS spectra of Pd 3d for PCNFs [17].

The electrodes modified with PCNF showed significantly increased electrocatalytic activity for glucose oxidation, exhibiting significantly reduced overpotential (0.32 V) and ultrafast (1 s) and sensitive current response with lower detection limits. It is believed that our process will provide an ideal platform for the large-scale design and construction of efficient biosensors and electrocatalysts [17].

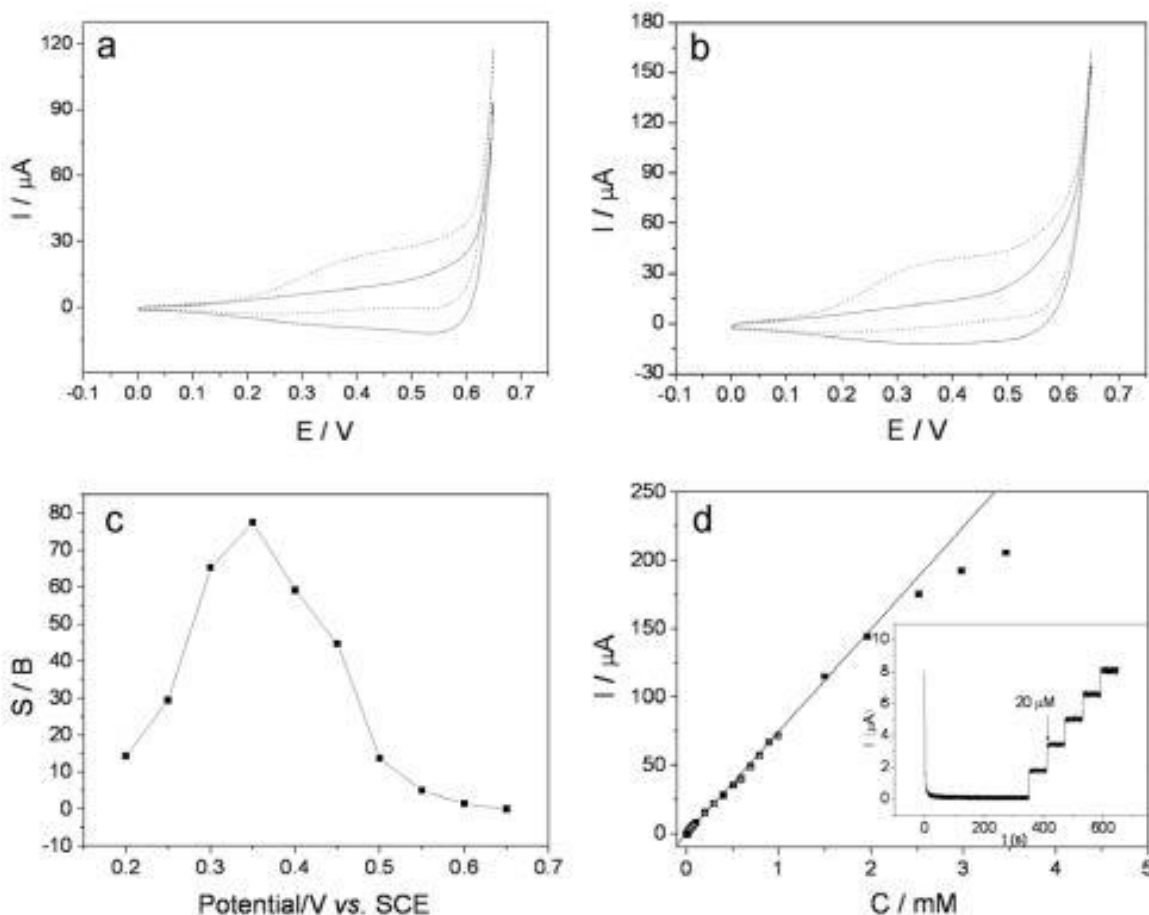


Figure II.22 Cyclic voltammograms (CVs) of 0.6 mM glucose in 0.1 M NaOH at the (a) pure CuO nanofibers modified and (b) PCNFs modified electrodes. Solid and dashed curves represent the CVs without and with glucose, respectively. The scan rate is 50 mV s^{-1} . (c) Plots of signal-to-background ratio to the applied potential on PCNFs modified electrode. (d) Calibration curve of glucose on PCNFs modified electrode. [17].

As comparison, and from the researches mentioned above, different types of CuO nanostructures are studied by a simple synthesis process, for used in glucose sensors (Table II.2). All CuO electrodes demonstrated the present glucose response in the oxidation process. The results indicate that the self-assembled CuO8 with a petal-like nanostructure is an interesting material due to its very high glucose sensitivity and selectivity. The Nafion/CuO8/GCE electrode showed excellent sensitivity to glucose at low concentrations.

Table II.2. A performance comparison of CuO thin films.

Electrode	Methods	Sensitivity ($\mu\text{A cm}^{-2}\text{mM}^{-1}$)	Linear range	Response time (s)	Detection limit	Ref
CuCo-CFs	electrospun nanofibers	507	0.02-11 mM	2s	-	3
Nafion/CuO8/GCE	electrochemical	7546.37	0.5 μM- 25.5 μM	1-2 s	0.25 μM	4
CuO/ZnO/FTO	Solution Process	1142	Up to 7	~1.5	-	13
CuO/NiO	Plasma	1103	1.65 mM	-	-	14
CuO-ZnO NRs/FTO	Solution Process	2961.8	0.001 μM - 8.45mM	<2	0.40 μM	15
CuO-NiO microfibers	electrospinning and calcination	3165.53	3 μM -0.51 mM	3s	0.001 μM	16
CuOnanofibers /Pd (IV)	electrospinning	1061.4	0.2 μM to 2.5 mM	1s	1.9*10 ⁻⁸ M	17



References

- [1] E.-H.Yoo, S.-Y.Lee, «*Glucose Biosensors: An Overview of Use in Clinical Practice*», journal/sensors, 10 (2010) 4558-4576.
- [2] L. Szablewski, «*Glucose Homeostasis – Mechanism and Defects*», Medical University of Warsaw Poland, (2015).
- [3] A. Senthamizhan, B. Balusamy, T.Uyar, « *Glucose sensors based on electrospun nanofibers: a review*», Anal Bioanal Chem, (2015) 1-22.
- [4] X. Wang, C.-y. Ge, K. Chen, Y.X. Zhang, « *An ultrasensitive non-enzymatic glucose sensors based on controlled petal-like CuO nanostructure*», Electrochimica Acta, (2017) 1-27.
- [5] H.Lee, Y. J. Hong, S. Baik, T. Hyeon, D. Kim, « *Enzyme-Based Glucose Sensor: From Invasive to Wearable Device*», Advanced Science News (2018).
- [6] H. W. Guggenheimer, «The Jerusalem Talmud, First Order: Zeraim», Tractate Berakhot, Chapter 1. מאימת, Published by De Gruyter, 18 (2000). <https://doi.org/10.1515/9783110800487.39>
- [7](<https://www.alamy.com/glucose-dextrose-d-glucose-molecule-linear-form-structural-chemical-formula-and-molecule-model-vector-illustration-image232783080.html>)
- [8] J. Vetelino, A. Reghu, « *Introduction to sensors*», Introd. To Sensors. (2011) 1–180.
- [9] V. Vinoth, T. Daliya, A.M. Asiri, J.J. Wu, «*Materials Science in Semiconductor Processing Facile synthesis of copper oxide micro flowers for non-enzymatic glucose sensor applications*», Mater. Sci. Semicond. Process. 82 (2018) 31–38.
- [10] M. Taguchi, A. Ptitsyn, S. Eric, J.C. Claussen, « *Nanomaterial-mediated Biosensors for Monitoring Glucose*», Journal of Diabetes Science and Technology, (2014) 1-9.
- [11] S. Laidoudi, M. Redha Kalledi, L. Lamiri, O. Belgherbi, S. Boudour, C. Dehchar, R. Boufnik, « *Non-enzymatic glucose detection based on cuprous oxide thin film synthesized via electrochemical deposition*», Applied Physics A (2021) 1–11.

- [12] S. Liu, W. Zeng, Q. Guo, Y. Li, « *Metal oxide-based composite for non-enzymatic glucose sensors*», J. Mater. Sci. Mater. Electron. 31 (2020) 16111–16136.
- [13] C.-E.Cheng, S. Tangsuwanjinda, H.-M. Cheng, P.-H. Lee, «*Copper Oxide Decorated Zinc Oxide Nanostructures for the Production of a Non-Enzymatic Glucose Sensor*», Coatings, 11 (2021) 1-10.
- [14] M.Palmer, M. Masikini, L.-W. Jiang, J.-J. Wang, F. Cummings, M. Chowdhury, «*Dataset of N-doped CuO: NiO mixed oxide thin film sensor for glucose oxidation*», Data in Brief, (2020) 1-16.
- [15] R. Ahmad, N. Tripathy, M.-S. Ahn¹, K. S. Bhat, T. Mahmoudi¹, Y. Wang, J.-Y. Yoo, D.-W. Kwon, H.-Y. Yang, Y.-B. Hahn, «*Highly Efficient Non-Enzymatic Glucose Sensor Based on CuO Modified Vertically-Grown ZnO Nanorods on Electrode*», Scientific Reports (2017) 1-10.
- [16] F. Cao, S. Guo, H. Ma, G. Yang , S. Yang, J. Gong, « *Highly sensitive nonenzymatic glucose sensor based on electrospun copper oxide-doped nickel oxide composite microfibers*», Talanta 86 (2011) 1-7.
- [17] W. Wang, Z. Li, W. Zheng, J. Yang, H. Zhang, C. Wang , « *Electrospun palladium (IV)-doped copper oxide composite nanofibers for non-enzymatic glucose sensors*», Electrochemistry Communications, 11(2009) 1-4.

Conclusion

Conclusion

Conclusion

During this work, we have found that the field of glucose sensing can develop rapidly through the use of the latest and greatest nanoscale metals, which have been widely introduced by researchers. Also, this research briefly summarized the difference between enzymatic and non-enzymatic glucose sensors. In addition, the properties of copper oxide films and the roles of different species were demonstrated. CuO has the best performance due to its high sensitivity, low detection limit, good stability and fast response time, which has made it possible to introduce these oxides as electrodes in non-enzymatic glucose sensors.

Finally, according to all the experimental results of our study and following a comparison of some electrocatalytic parameters of the proposed sensor with several glucose sensors reported by the researchers, we concluded that the self-assembled CuO8 with a petal-like nanostructure is an interesting material due to its very high sensitivity and selectivity to glucose. The Nafion/CuO8/GCE electrode showed excellent sensitivity of $7546.37 \mu\text{A mM}^{-1} \text{cm}^{-2}$ and a low detection limit of $0.25 \mu\text{M}$.

Abstract

Copper oxide is one of the most important semiconductors in modern technological and scientific applications. It has received great attention for its wide use in many applications such as chemical sensors, catalysts and other technological applications. Copper oxide CuO has a low band gap varied between 1.2 eV and 1.9 eV, and is also characterized by its unique and specific properties which allowed us to use it as an electrode in glucose sensors. In this work and according to the results obtained, the nanostructures of copper oxide in the form of the petals are characterized by an extremely high sensitivity, a selectivity in glucose and a good stability. The best results showed a high sensitivity of $7546.37 \mu\text{A}/\text{mM}\times\text{cm}^2$ with a low detection limit of $0.25 \mu\text{M}$.

Key-words: Copper oxide, glucose sensors, sensitivity, detection limit.

Résumé

L'oxyde de cuivre est l'un des semi-conducteurs les plus importants dans les applications technologiques et scientifiques modernes. Il a reçu une grande attention pour sa large utilisation dans de nombreuses applications telles que les capteurs chimiques, les catalyseurs et d'autres applications technologiques. L'oxyde de cuivre CuO possède une faible bande interdite comprise entre 1,2 eV et 1,9 eV, et également se caractérise par ses propriétés uniques et spécifiques ce qui nous a permis de l'utiliser en tant que électrode aux capteurs de glucose. Dans ce travail et selon les résultats obtenus, les nanostructures de l'oxyde de cuivre sous forme des pétales sont caractérisées par une sensibilité extrêmement élevée, une sélectivité en glucose une bonne stabilité. Les meilleurs résultats ont montré une sensibilité élevée de $7546.37 \mu\text{A}/\text{mM}\times\text{cm}^2$ avec une limite de détection faible de $0,25 \mu\text{M}$.

Mots-clés : oxyde de cuivre, capteurs de glucose, sensibilité, limite de détection.

ملخص

يعتبر أكسيد النحاس من أهم أشباه الموصلات في التطبيقات التكنولوجية والعلمية الحديثة، وقد حظي باهتمام كبير لاستخدامه الواسع في العديد من التطبيقات مثل المستشعرات الكيميائية والمحولات والتطبيقات التكنولوجية الأخرى. يحتوي أكسيد النحاس CuO على فجوة نطاق منخفضة تتراوح بين 1.2 فولت و 1.9 فولت، ويتميز أيضاً بخصائصه الفريدة والمحددة التي سمحت لنا باستخدامه كقطب كهربائي في مستشعرات الجلوكوز. في هذا العمل وفقاً للنتائج التي تم الحصول عليها، تتميز الهياكل النانوية لأكسيد النحاس على شكل بتلات بحساسية عالية للغاية وانتقائية في الجلوكوز واستقرار جيد. أظهرت أفضل النتائج حساسية عالية 7546.37 ميكرو اومبير / مم × سم² مع حد اكتشاف منخفض قدره 0.25 ميكرومول.

الكلمات المفتاحية: أكسيد النحاس : مستشعرات الجلوكوز , حساسية , حد اكتشاف.